Project title:	Effect of regular watercress consumption during radiotherapy treatment for early stage breast cancer
Project number:	FV 433
Project leader:	Dr Jonathan Swann, University of Reading
Report:	Final report, November 2016
Previous report:	Annual report, October 2015
Key staff:	Natasa Giallourou, PhD student
Location of project:	Reading, UK
Industry Representative:	Dr Steve Rothwell, Vitacress salads Ltd
Date project commenced:	October 2013
Date project completed (or expected completion date)	October 2016

DISCLAIMER

While the Agriculture and Horticulture Development Board seeks to ensure that the information contained within this document is accurate at the time of printing, no warranty is given in respect thereof and, to the maximum extent permitted by law the Agriculture and Horticulture Development Board accepts no liability for loss, damage or injury howsoever caused (including that caused by negligence) or suffered directly or indirectly in relation to information and opinions contained in or omitted from this document.

AUTHENTICATION

We declare that this work was done under our supervision according to the procedures described herein and that the report represents a true and accurate record of the results obtained.

Daniel Commane

Lecturer

University of Reading

Signature ..... Date .....

Jonathan Swann

Senior Lecturer

Imperial College London

Signature ..... Date .....

CONTENTS

GROWER SUMMARY

Headline

- Novel anti-cancer properties have been identified for watercress and a watercress-derived compound phenethyl isothiocyanate (PEITC).
- *In vitro* studies show that PEITC enhances the effects of radiotherapy on breast cancer cells and that watercress extract protects healthy cells from the side-effects of radiotherapy.

Background

Breast cancer is a leading cause of cancer-related mortalities globally and epidemiological studies suggest a strong link between healthy nutrition and cancer prevention. Members of the Brassicaceae family like watercress have been extensively studied for anti-cancer properties. Watercress has a complex phytonutrient profile characterised by high levels of carotenoids, flavonols and glucosinolates which all have proven health benefits. Extracts of watercress exhibit strong antioxidant capacity in cells. Watercress and its components have been associated with the inhibition of the three stages of carcinogenesis: initiation, proliferation and metastasis in cancer cell models. Phenethyl isothiocyanate (PEITC) is a glucosinolate breakdown product and watercress is the richest dietary source of it. It has received considerable attention for its anti-cancer properties and has been tested in a number of clinical trials with promising outcomes.

In this study we examined the effect of crude watercress extract and PEITC on breast cancer and healthy breast cells focussing on cancer metabolic pathways as well as DNA damage levels. Radiotherapy is the most common treatment modality for breast cancer patients and functions by killing cancer cells but simultaneously affecting healthy tissue with marked incidents of skin dermatitis. We therefore, proceeded to examine the potential synergistic effect of irradiation exposure and watercress as well as PEITC against breast cancer cells and further investigated whether watercress or PEITC can be protective against radiation-induced collateral damage.

Watercress is becoming increasingly popular in modern cuisines, mainly as a salad crop but also in soups, smoothies and other cooked dishes. We therefore looked at the impact of common cooking methods on the phytonutrient profile of watercress in order to give recommendations on the most appropriate way of preparation.

The aims of the project were to:

1. Investigate the impact of watercress and PEITC on the metabolome (collection of metabolites) of breast cancer and healthy breast cells.
2. Evaluate the interactions between watercress or PEITC with ionising radiation, on markers of cellular function and the metabolism of breast cancer and healthy breast cells.
3. Examine the effects of domestic cooking methods on the phytochemical profile of watercress and formulate recommendations for optimal preparation to maximise nutrient ingestion.

Summary

The impact of watercress and PEITC in cancer and healthy cells

We performed cell cycle experiments that helped us understand at which point of the cancer cell's life cycle can watercress and PEITC inhibit growth and proliferation. Cell cycle can be seen as the quality control station in the life of a cell. If a cell fails this control it initiates its suicide processes. The earlier the watercress or PEITC stop the cell cycle, the better the chances of cancer cell death are. Our results suggest that watercress and PEITC cause a significant dose dependant arrest in the cancer cell's life cycle without having a major impact in healthy cells.

DNA damage is a very important step in cancer initiation and progression. The higher the level of DNA damage in a cancer cell the better the chances of the cell undergoing programmed cell death (apoptosis). PEITC contributes to cancer cell death by depleting the cells of their major antioxidant molecule, glutathione, increasing the amounts of harmful reactive oxygen species inside the cells and essentially increasing the levels of DNA damage, leading to cell death. Watercress extract does not cause DNA damage to cancer cells but affects their antioxidant status and significantly limits the cancer cells' nutrient and energy sources necessary for cell proliferation and survival. PEITC on the other hand is highly damaging to cancer cells but it also harms healthy cells at high doses (Figure i).

Figure (i) DNA damage levels from effects of the crude watercress extract and PEITC on cancer cells (A&B) and healthy cells (C&D) after a 24-hour treatment. Statistically significant differences between control and treated cells are indicated *p<0.05, ***p<0.001). Data shown represent the average of three independent experiments + SEM with two replicates per sample. WX, watercress.

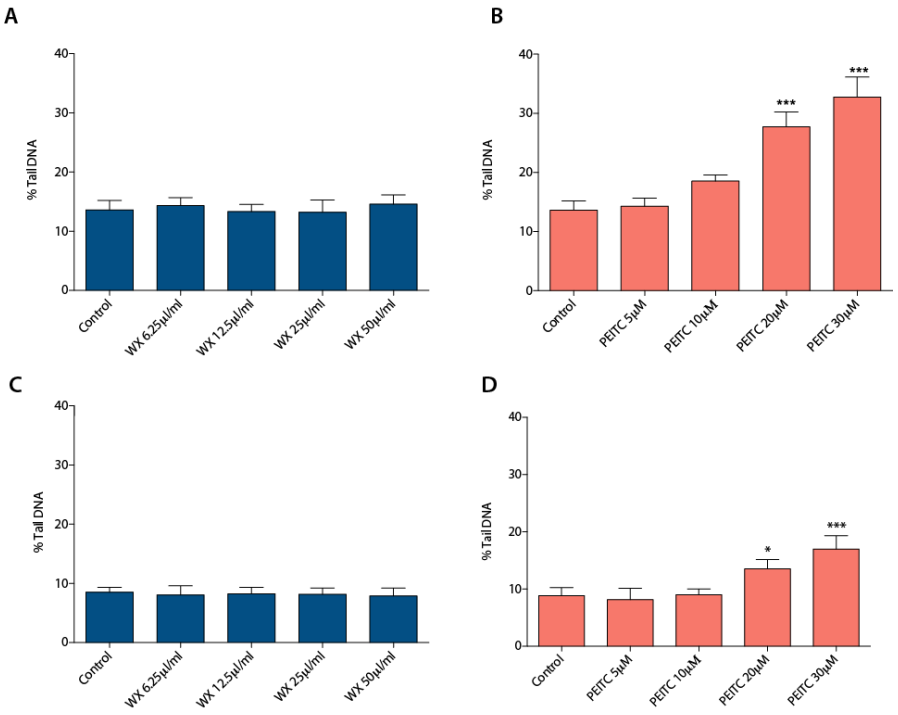

The combined effect of watercress or PEITC with radiation treatment in cancer and healthy cells

To mimic the conditions of radiotherapy during breast cancer in real life we irradiated cancer and healthy cells that had previously been treated with either PEITC or watercress extract. The results from the radiation experiments suggest that PEITC causes additional DNA damage and cell cycle arrest in cancer cells adding to the irradiation induced cancer-killing process. The fact that PEITC is depleting cancer cells of their major antioxidant renders these cells prone to damage such that they cannot survive the cancer killing effects of irradiation. Pre-treatment of the healthy cells with the watercress extract reduces DNA damage levels caused by irradiation, by up-regulating these cells' antioxidant mechanisms as observed by increased glutathione levels in these cells (Figure ii).

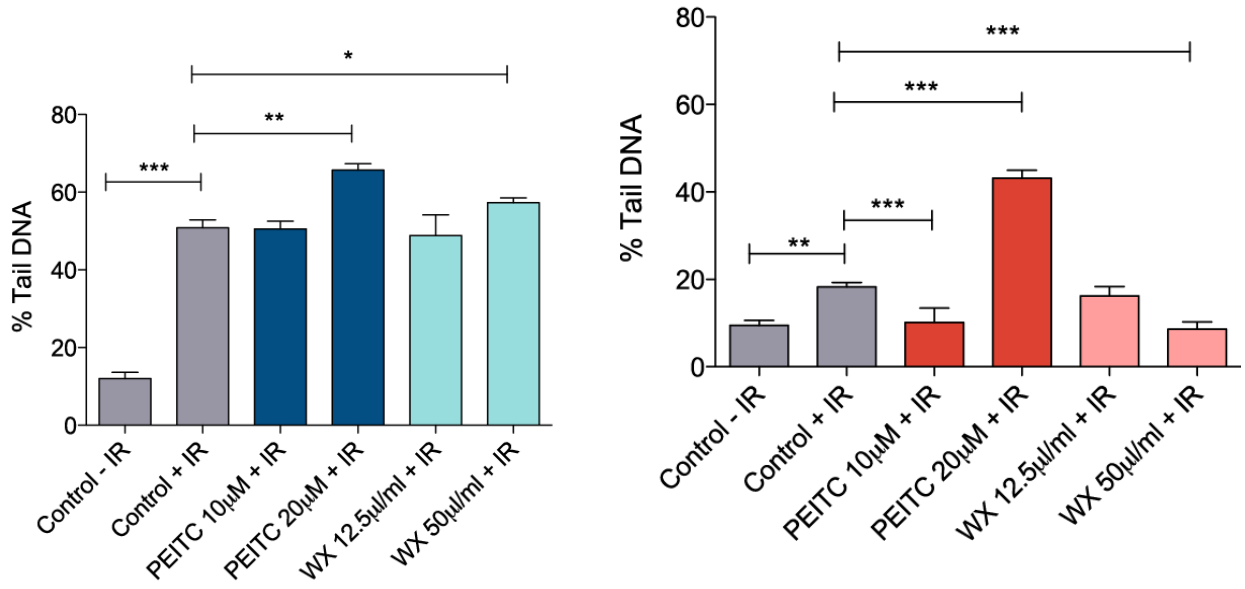

CANCER CELLS **HEALTHY CELLS**

Figure (ii) DNA damage levels in cancer and healthy cells exposed to 5 Gy of IR following 24 hour pre-treatment with PEITC or crude watercress extract (WX). Statistically significant differences between groups are indicated as follows *p<0.05, **p<0.01, ***p<0.001. Data shown represent the average of three independent experiments + SEM with two replicates per sample. In 'Control – IR' treatments, cells were not irradiated and not pre-treated with watercress or PEITC; in 'Control + IR' treatments, cells were irradiated but not pre-treated with watercress or PEITC.

Overall, *in vitro* studies indicated that PEITC can enhance the sensitivity of cancer cells to irradiation making the cancer killing process more effective, and watercress extract can protect healthy breast cells from radiation-induced damage.

Effect of cooking on watercress nutrients

The impact on the phytonutrient profile of five different common watercress preparation methods was examined namely, microwaving, steaming, boiling, chopping as well as blending into a smoothie. In the experiments performed, changes in the phenolic, carotenoid and glucosinolate content were quantified as well as the overall antioxidant activity. Our results suggest that microwaving and steaming ensure better retention of all the phytonutrients measured. On the other hand, boiling has detrimental effects on the levels of phytonutrients and should be avoided to ensure maximum ingestion of beneficial compounds.

Limitations

One limitation of this study is that our results have not been validated in a human trial where breast cancer patients would consume watercress during their radiotherapy treatment. Our experiments in breast cells provide a substantial body of evidence for the potential efficacy of watercress against radiation-induced damage. Future work that includes the performance of a human clinical trial with watercress as a nutritional intervention is highly recommended. Dietary guidance is very limited during radiotherapy therefore such a study could generate useful information for the efficacy of antioxidant diets against damage.

Financial Benefits

There are no financial benefits for growers at this stage. However, if further *in vivo* studies are conducted and reported that support the results of these *in vitro* studies, then growers may see increased growth in watercress sales.

Action Points

None to date

SCIENCE SECTION

Introduction

Watercress (*Nasturtium officinale*) belongs to the family of Brassicaceae together with broccoli, Brussels sprouts and kale. Epidemiological studies suggest a link between the consumption of Brassica vegetables and a reduced risk for many types of cancers (Verhoeven *et al*., 1996) including breast cancer (Boggs *et al*., 2010, Liu and Lv, 2013). Watercress has a complex phytochemical profile characterised by high levels of carotenoids, flavonols and glucosinolates (Giallourou *et al*., 2016). Extracts of watercress exhibit strong antioxidant capacity *in vitro* (Gill *et al*., 2007, Fogarty *et al.*, 2013). Watercress and its components have been associated with the inhibition of the three stages of carcinogenesis: initiation, proliferation and metastasis in *in vitro* cancer cell models (Boyd *et al*., 2006, Rose *et al.*, 2005a, Rose *et al.*, 2000).

Plant tissue damage such as cutting or chewing, induces the release of the plant enzyme myrosinase (β-thioglucoside glycohydrolase; EC 3.2.3.1), which hydrolyses glucosinolates present, forming reactive isothiocyanates. It is this group of bioactive compounds that have received considerable attention for their potential anti-cancer properties. Watercress is particularly rich in gluconasturtiin, which is the glucosinolate precursor to phenethyl isothiocyanate (PEITC). Research has highlighted promising chemopreventive and chemotherapeutic activities of PEITC. Due to its highly electrophilic nature PEITC reacts with cellular thiols via thiocarbamoylation and after its cellular uptake it reacts with glutathione (GSH), which is the major intracellular antioxidant (Zhang, 2000, Zhang, 2001, Syed Alwi *et al*., 2012) depleting cells of their GSH content (Fig.1).

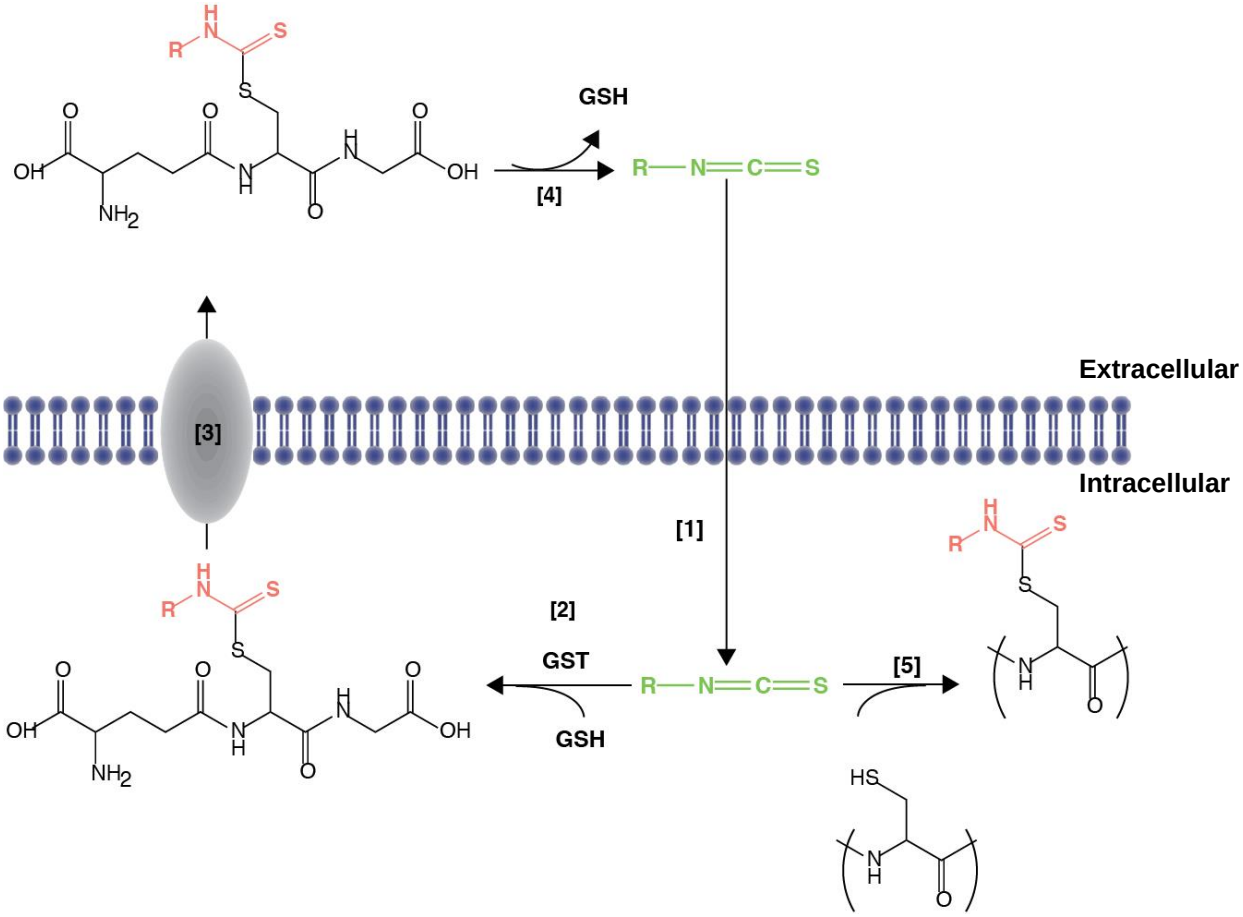

Figure 0. Intracellular accumulation of ICTs

Isothiocyanates diffuse across the plasma membranes (1) and once located in the intracellular space they bind to thiol groups in glutathione (GSH), upon the action of glutathione-S-transferase (GST) (2). The glutathione-isothiocyanate conjugate is then exported from the cells via efflux pumps (3). The conjugate is hydrolysed extracellularly (4) giving rise to a free isothiocyanate, which can then re-enter the cell. This cycle results in a rapid accumulation of isothiocyanates and the concurrent depletion of intracellular glutathione, allowing isothiocyanates to bind via thiol groups to other proteins (5) via thiocarbamoylation. Figure adapted from (Cavell *et al*., 2011).

GSH has a vital role in the maintenance of cellular redox status (Vaughn and Deshmukh, 2008). Tight regulation of intracellular reactive oxygen species (ROS) through the induction of antioxidant mechanisms is central to cancer cell survival. Low levels of ROS can have a proliferative advantage for cancer cells (Hu *et al*., 2005). Excessively high levels of ROS though, will result in disruptions in redox balance that can lead to mitochondrial damage underpinned by oxidative stress, and ultimately cancer cell death (Cairns *et al*., 2011). To manage this, cancer cells use antioxidants such as GSH, to prevent ROS from accumulating at detrimentally high levels. Malignant cells are commonly characterised by elevated ROS levels compared to non-cancerous cells (Hu *et al*., 2005). PEITC treatment has therefore a selective detrimental effect on cancer cells since they rely on their antioxidant mechanisms for survival and PEITC depletes the cellular levels of their main antioxidant, GSH.

Combined treatment of cancer cells with PEITC along with established chemotherapeutic agents such as cisplatin and doxorubicin potentiates their cancer-killing properties (Wang *et al.*, 2011, Eisa *et al*., 2015) providing preliminary evidence for the use of PEITC as an adjuvant treatment during radiotherapy in breast cancer patients. PEITC, due to its highly electrophilic nature reacts with cellular thiols via thiocarbamoylation. After its cellular uptake it also reacts with glutathione (GSH), the major intracellular antioxidant, depleting cells of their GSH content and impacting cell survival (Zhang, 2000, Zhang, 2001, Syed Alwi *et al*., 2012). As radiotherapy works primarily by inducing DNA damage through the formation of free radicals, the ability of PEITC to deplete the radical scavenger GSH is likely to contribute to its radio-sensitising properties.

At the cellular level PEITC has been extensively shown to have direct anti-cancer effects in *in vitro* cancer models. It causes cell cycle arrest in a wide variety of cell lines and it is a potent inducer of apoptosis (programmed cell death) (Syed Alwi *et al*., 2012, Cheung *et al*., 2008, Xiao *et al*., 2004). PEITC increases the activity of Nrf2, a key transcription factor relevant to the activation of oxidant/electrophile response genes mediating chemo-preventative functions (Xu *et al*., 2006). PEITC also inactivates the nuclear factor kappa B (NF-kB) pathway affecting important steps in carcinogenesis including, inflammation, cancer cell survival, differentiation and proliferation (Xu *et al*., 2005, Jeong *et al*., 2004, Karin, 2006). Inflammation is a central process in cancer development and PEITC has been shown to decrease the expression of inducible nitric oxide synthase (iNOS) and cyclooxygenase-2 (COX-2) resulting in an attenuated secretion of pro-inflammatory mediators (Rose *et al*., 2005b). Other targets of PEITC include the hypoxia inducible factor (HIF) (Wang *et al*., 2009) negatively regulating angiogenesis as well as inhibiting mTOR (mechanistic target of rapamycin), which plays a key anabolic role in translation and functions as a vital metabolic integration point joining nutrient availability with growth signals (Cavell *et al*., 2012, Cairns *et al*., 2011).

Metabolic regulation is a determining element of the cell growth machinery and cancer cells have adapted to several oncogenic signals to modify their metabolic phenotype as such, to support their needs for growth, survival and malignant transformation. Core cancer cell metabolism serves the three basic needs of proliferating cells: i) rapid ATP generation to sustain energy status, ii) increased need for the biosynthesis of macromolecules, proteins, lipids and nucleotides, iii) maintenance of appropriate cellular redox status.

To our knowledge, limited work has been done on the effects of PEITC and of crude watercress extract on cancer cell energetics and metabolism. PEITC impacts a great range of oncogenes and tumour suppressor genes, which can all cause shifts in intracellular

signalling pathways involved in cancer cell metabolism. It is therefore central to get an insight into the effect of such a bioactive compound on the global metabolic profile of cancer cells.

This project primarily investigated the biochemical response of MCF-7 breast cancer cells to increasing doses of watercress extract and to PEITC using ^{1}H NMR metabonomics. This was then compared to the metabolic response of immortalised but non-tumorigenic MCF-10A cells to the same treatments. Metabonomic observations were then related to inducible cancer related phenotypic changes in cell behaviour. On the basis of the results obtained from this work, the potential of watercress or PEITC to sensitise cancer cells to ionising radiation and/or their potential to protect healthy cells from collateral damage was examined.

Project framework

On the basis of the reviewed literature herein it is apparent that watercress and PEITC potentially modulate a range of factors implicated in cancer onset and progression and are influential in the efficacy of cancer treatment. Characterising the biochemical effects of watercress components and PEITC on cellular energetics is key to understanding the mechanisms through which they exert their beneficial effects. As such, a central aim of this project was to define the metabolic impact of watercress and PEITC exposures on breast cancer and healthy cells lines. Further we aimed to assess the potential of watercress and PEITC to act as radio-sensitising or radio-protective agents in breast tumour or normal cells respectively.

Aims

1. Investigate the impact of watercress and PEITC on the metabolome of breast cancer and healthy breast cells
2. Evaluate the interactions between watercress or PEITC with ionising radiation on markers of cellular function and metabolism of breast cancer and healthy breast cells
3. Examine the effects of domestic cooking methods on the phytochemical profile of watercress and formulate recommendations for optimal preparation to maximise nutrient ingestion

The initial plan for this project included the performance of a human clinical trial investigating the impact of watercress consumption in breast cancer patients undergoing radiotherapy. For the purposes of this project, plasma and urine samples obtained from the patients would have been analysed using ^{1}H NMR spectroscopy to profile the metabolic phenotypes of the patients before and after radiotherapy. This would have allowed for the biochemical modifications associated with radiotherapy to be explored and the ability of watercress to modulate such

responses to be elucidated. This study was intended to take place at the University Hospital of Santa Maria in Lisbon and funded by VITACRESS Portugal. Unfortunately due to insufficient number of participants recruited, the study was significantly underpowered and therefore no meaningful and solid scientific data were generated. Therefore, we proceeded in designing the *in vitro* experiments mentioned above.

Materials and methods

Cell Culture

The MCF-7 human breast adenocarcinoma cell line was purchased from the American Type Culture Collection (ATCC) (LGC standards, Middlesex, UK). Cells were cultured in Dulbecco's Modified Eagle's Medium (DMEM; Lonza Group Ltd, Basel, Switzerland) supplemented with 10% (v/v) foetal bovine serum (FBS; Lonza Group Ltd), 2 mM glutamine (Thermo Fisher Scientific, Loughborough, UK), 50 U/ml penicillin and 50 U/ml streptomycin (Thermo Fisher Scientific, Loughborough, UK) and 1% non-essential amino acids (Sigma-Aldrich, Dorset, UK).

The MCF-10A, non-tumorigenic breast epithelial cell line was kindly provided from Prof. Graham Packham (University of Southampton, Southampton, UK). Cells were maintained in Ham's F12:DMEM (1:1) (Lonza Group Ltd), 20 ng/ml epidermal growth factor (EGF) (PeproTech, London, UK), 0.1 µg/ml cholera toxin (Sigma-Adrich), 10 µg/ml insulin (Invitrogen), 500 ng/ml hydrocortisone (Sigma-Aldrich), 5% horse serum (Invitrogen) and 50 U/ml penicillin and 50 U/ml streptomycin (Thermo Fisher Scientific, Loughborough, UK).

Cells were grown in an incubator at 37 ºC with 5% CO_2 and 95% humidity in 75 cm^2 culture flasks and were routinely passaged at approximately 70% confluency. The medium was changed every 2-3 days. For passaging, cells were washed with phosphate buffer saline (PBS; Lonza Group Ltd) before detaching with 5 ml of Trypsin-Versene® (EDTA) mixture (Lonza Group Ltd) for 3-5 min for MCF-7 cells and 18-20 min for MCF-10A cells. Media (5 ml) was then added to the cells to inactivate the trypsin and the cell suspensions were centrifuged at 300 *g* for 3 min. Cell pellets were re-suspended in complete media in the flask and incubated.

Compounds and Extracts

Analytical grade compounds

Phenethyl isothiocyanate (PEITC) was purchased from Sigma (Dorset, UK). PEITC stock solution (30 mM) was made up in DMSO fresh on the day of use.

Watercress extracts

Fresh watercress samples were obtained directly from Vitacress Salads Ltd. (Andover, UK). Samples were snap frozen in liquid nitrogen and stored at -80 ºC. 2 g of leaf and 2 g of stem were weighed and placed in a 20 ml syringe (BD Biosciences, Oxford, UK) that had had the plunger removed and a circular 25 mm glass microfiber filter (Whatman, Dassel, Germany) placed at the bottom. The syringe was then placed inside a 50 ml centrifuge tube without the lid and centrifuged at 1500 *g* for 30 min to collect the extract. This crude watercress extract was then filtered through a 0.22 µm filter and used in the cultures.

Irradiation

MCF-7 and MCF-10A cells were plate seeded in the respective culture plates for each experiment and next day were treated with the crude watercress or PEITC for 24 hours. At the end of the treatment period the cells were exposed to 5 Gy X-ray radiation using an orthovoltage X-ray unit (Gulmay Medical D3225, Xstrahl, UK). The irradiator was at a stable fixed distance from the cell culture plates and the irradiator field was approximately 20 x 20 cm. The cell culture plates were placed in the centre of the irradiation field.

Following radiation treatment cells were returned in the incubator and were allowed to rest for 1 hour. The cells were then collected and used in the experiments.

Cell viability

Cell viability was assessed using the MTT (3-[4,5- dimethylthiazol-2-yl]-2,5-diphenyl tetrazolium bromide) based *in vitro* toxicology assay kit (Sigma-Aldrich, Dorset, UK) according to the manufacturer's instructions. Briefly, $5x10^3$ MCF-7 or MCF-10A cells were seeded in 96 well plates. Cells were allowed to attach overnight and were then treated with PEITC (10, 20 µM) or the watercress extract (12.5, 50 µl/ml) for 24 hours. Three hours before the end of the treatment duration cell were irradiated and allowed to rest as described above. Two hours before the end of duration of the treatment MTT solution was added to each well equal to 10% of the culture medium volume and the cells were incubated for the remaining 2 hours. Following MTT incubation, the formazan crystals formed were dissolved in MTT solubilisation solution equal to the original culture medium volume. Plates were shaken to enhance dissolution and absorbance was measured at 570 nm and 690 nm (background absorbance)

Cell proliferation

For the determination of cell proliferation MCF-7 and MCF-10A cells were seeded in 96-well microplates at $5x10^3$ cells per well and incubated at 37 ºC with 5% CO_2 and 95% humidity for 24 hours. Cells were exposed to the watercress extract at 6.25, 12.5, 25 and 50 µl/ml and PEITC at 5, 10, 20, 30 µM for 24 hours. The treatments were then removed by aspiration.

Cells were permeabilised with 100 µl of ice-cold methanol for 5 min at room temperature. Methanol was removed and the plates were allowed to air dry for 15 min in a hood, followed by addition of 100 µl of DAPI in PBS (70 µl of 30mM DAPI stock solution in 10.43 ml of PBS). Cells were incubated in the dark for 30 min at 37 ºC and absoprtion was measured using GENios microplate reader (TECAN Group Ltd., Mannedorf, Switzerland) with absorbance at 340 nm and emission at 465 nm. The experiment was performed in triplicate with three technical replicates per experiment.

NMR Metabonomics

The metabolic profiles of MCF-7 and MCF-10A cells were analysed using ^{1}H NMR spectroscopy. Cells were seeded at $1x10^{5}$ cells per well into six well plates and treated at 80% confluency. Cells were exposed to the watercress extract at 6.25, 12.5, 25 and 50 µl/ml and PEITC at 5, 10, 20, 30 µM for 24 hours. Media was transferred into eppendorf tubes and cells on the surface of the plate were washed twice using 1 ml cold (4ºC) PBS and were quenched using 1 ml of ice-cold methanol (maintained on dry ice). Cells were allowed to lyse for 2 mins and were detached from the plate using a cell scraper and transferred into an Eppendorf tube. Methanol quenching was repeated to maximise metabolite recovery. A vacuum concentrator (SpeedVac) was used to dry down the cell suspensions before reconstitution in 80 µl of phosphate buffer (pH 7.4) in 100% deuterium oxide containing 1 mM of the internal standard, 3-(trimethylsilyl)-[2,2,3,3,-$^{2}H_{4}$]-propionic acid (TSP).

For every sample, a standard one-dimensional NMR spectrum was acquired using a 600 MHz Bruker NMR spectrometer, with water peak suppression using a standard pulse sequence (recycle delay (RD)-90°-t1–90°-tm-90°-acquire free induction decay (FID)). For each spectrum 256 scans and 8 dummy scans were obtained, collected in 64K data points with a spectral width of 12.001 ppm. ^{1}H NMR spectra were manually corrected for phase and baseline distortions and referenced to the TSP singlet at δ 0.0. Spectra were digitized using an in-house MatLab (version R2012a, The Mathworks, Inc.; Natwick, MA) scripts. Metabolites were using an in-house database of standards and Chenomx NMR suite (version 7.7, Chenomx Inc). Multivariate modelling, including principal component analysis (PCA) and orthogonal projections to latent structures discriminant analysis (OPLS-DA), was performed on the samples using in house scripts

Cell Cycle

Cell cycle can be considered as the life cycle of a cell and it involves a series of stages and checkpoints (‘quality-control points’) that ensure nutrient supply is adequate and that DNA damage levels are not hindering proliferation. Increase in the proportion of cancer cells at any

of the stages of cell cycle suggests growth and proliferation arrest that can essentially result in cancer cell death.

MCF-7 and MCF-10A cells were seeded at a $1x10^5$ cells per well in six well plates and incubated as required. The cells were then exposed to the watercress extract and PEITC at 6.25, 12.5, 25, 50 µl/ml and 5, 10, 20, 30 µM, respectively for 24 hours. Following treatment removal, the cells were washed with cold PBS (4°C) and harvested by trypsinisation. Cells were pelleted by centrifugation at 300 *g* for 3 min and the supernatant was discarded. The cell tissue was then re-suspended in 200 µl of cold PBS and fixed with drop-wise addition of 70% (v/v) fresh ice-cold methanol. The samples were then stored at -20 °C until analysis.

On the day of the analysis, samples were centrifuged at 300 *g* for 3 min and the supernatants were discarded. The cell pellets were then re-suspended in 200 µl of PBS and 25 µl of 1 mg/ml RNAse was added to the suspensions. The samples were incubated at 37°C for 30 min and 2.5 µl of 400 µg/ml of PI dye were added to the cells which were then incubated for a further 30 min at room temperature under dark conditions. The final volume of the cell suspensions was adjusted to 600 µl with PBS. Cellular DNA content of 15,000 cells was quantified via flow cytometry. The flow cytometry analysis was performed using the FL2 channel on a BD Accuri™ C6 flow cytometer (Germany). Data analysis was facilitated using the Flow Jo software (version 7.6, Tree star Inc, Oregon, USA). Cell cycle progression was evaluated accounting for the percentage of cells in each of the phases Gap0/1 (G0/1), Synthesis (S), Gap2/mitosis (G2/M) and apoptotic cells (sub G0/1). The principle of the cell cycle analysis is based on the fluorescence intensity of the PI nuclear dye that is proportional to the DNA concentration of the cell.

Comet Assay

The Comet assay is used to for the measurement of DNA strand breaks in single cells, signifying levels of DNA damage. MCF-7 and MCF-10A cells were seeded in T25 cells culture flasks at a concentration of $1x10^6$ and maintained at 37 °C with 5% CO_2 and 95% humidity. The cells were then exposed to the watercress extract and PEITC at 6.25, 12.5, 25, 50 µl/ml and 5, 10, 20, 30 µM, respectively for 24 hours. The treatment solutions were then removed via aspiration followed by washing with PBS and detaching from the cell culture flask with trypsin. Cell suspensions were adjusted to a concentration of $1x10^6$ cells/ml.

Following the treatments, 50 µl of the cell suspensions were centrifuged at 300 *g* for 5 min at 4°C. The supernatants were discarded and the cell pellets were re-suspended in 85 µl of warm low melting point agarose (0.85% w/v) and applied on fully frosted microscope slides pre-coated with two layers of normal melting point agarose (1%). The slides were cooled at 4 °C for 5 min before adding a second layer of 150 µl LMA and allowed to solidify at 4 °C for

10 min. The slides were then transferred into a staining jar, lysis buffer was added (2.5 M NaCl, 0.1 M EDTA, 0.01 M Tris and 1% (v/v) Triton X – added just prior to use – pH 10), and the cells were lysed for 1 hour at 4 °C).

Following lysis of the cells, the slides were placed in a horizontal electrophoresis tank and incubated for 20 min in alkaline buffer (0.3 M NaOH, 1 mM EDTA – pH 13) at 4 °C in dark conditions. Subsequent to DNA unwinding, electrophoresis was carried out at 26 V, 300 mA for 20 mins at 4 °C. Immediately after electrophoresis the slides were washed in neutralising buffer (0.4 M Tris – pH 7.5) three times for 5 min.

Slides were stained with ethidium bromide (20 µl/ml) and DNA migration from the nucleus was visualised with a fluorescence microscope (Olympus). The computer-based image analysis software, Komet 4.0 (Andor Technology, South Windsor, CT) was used to calculate a number of parameters associated with DNA damage. These included % tail DNA, the proportion of DNA migrated from the head to the tail of the comet; tail length, the distance (µm) of DNA from the nucleoid core; extent tail moment, an index of DNA damage that considers both the tail length and the fraction of DNA in the comet tail (extent tail moment = % tail DNA x tail length/100); and olive tail moment, an index of DNA damage that represents the product of %tail DNA and the distance between the centres of gravity of the head and the tail regions of a comet, [olive tail moment = (tail centre of gravity – head centre of gravity)* % tail DNA/100]. The mean value from 75 randomly scored cells was taken as an index of damage for each replicate well.

Mitochondrial membrane potential assay

Enzymatic activity in the electron transport chain generates a potential across the mitochondrial membrane. A hallmark of cell apoptosis is the collapse of the mitochondrial membrane potential accompanied by the opening of the mitochondrial permeability transition pores that in turn releases cytochrome c which then triggers a range of apoptotic events. This assay is therefore used as a marker of cancer cell apoptosis (programmed cell death). Mitochondrial membrane potential was assessed according to the JC-10 mitochondrial membrane potential kit according to the manufacturer's instructions. Briefly, $1x10^4$ MCF-7 and MCF-10A cells were seeded in a 96 well plate and allowed to attach overnight. The cells were then exposed to the watercress extract at 6.25, 12.5, 25 and 50 µl/ml and PEITC at 5, 10, 20, 30 µM for 24 hours. JC-10 dye-loading solution (50 µl) was added to each well and incubated for 60 min before measuring fluorescent intensities (Ex/Em= 485/520 nm and Ex/Em=544/590 nm). The shifts of mitochondrial membrane potential were measured as the ratio between aggregate (Em =520 nm) and monomeric forms (Em =590 nm) of the JC-10

dye using FLUOstar Omega (Isogen Life Science, De Meer, the Netherlands). Increasing ratio indicates mitochondrial membrane depolarization

Univariate statistical analyses

Statistical analyses for all experiments excluding 1H NMR metabonomics were performed using GraphPad Prism version 5.0a for Mac OS X, La Jolla, California, USA). Statistical significance was obtained using one-way analysis of variance (ANOVA) and the Bonferroni post-hoc test.

Materials and methods for watercress domestic processing experiments

Plant Material

Fresh watercress samples were provided from VITACRESS LTD (Andover, Hampshire, UK), transferred to the laboratory and stored at 4 °C for up to 24 hours until all watercress processing analyses were performed. Only samples free from mechanical damage were used in the experiments. All analyses were performed in triplicate using the same batch of plant material to minimise variation in our results.

Reagents & Chemicals

All chemicals were obtained from Sigma Aldrich (Poole, UK), unless otherwise stated.

Domestic Processing

The effect of domestic processing on the phytochemical content and antioxidant activity of watercress was examined by cooking of the plant material by boiling, microwaving, steaming, chopping and blending with water to make a watercress smoothie. Processing treatments and cooking times used were based on general consumer preferences and after online searches of watercress recipes as well as using past research papers looking at the effects of domestic processing in other types of Brassica vegetables. 100 g portions of watercress were used for each replicate *(n=3).* Temperature data for boiling and steaming treatments were recorded throughout cooking, using a temperature logger (Squirrel OQ610-S, Grant instruments, UK) and a type T thermocouple.

Boiling *(n=3):* 500 ml of tap water was brought to boil (90 °C) in a stainless steel pot and watercress was boiled for 2, 5 and 10 min. Watercress was removed from the boiling water and was kept at -20 °C for analysis.

Microwaving *(n=3):* Fresh watercress was placed in plastic trays, then transferred to a domestic microwave oven (Panasonic, UK) and cooked at full power (1400 W) for 1, 2 and 3 min.

Steaming *(n=3):* A domestic steamer (Russel Hobbs, UK) was pre-heated at 100 °C with 500 ml water at its base. Watercress was placed in the steamer and cooked for 5, 10 and 15 min.

Chopping *(n=3):* 100 g of watercress was transferred to a food processor (Waring Commercial, New York, USA) and chopped for 30 secs at full speed. To study the effect of storage time on the phytochemical content, the chopped watercress was left on the bench at room temperature (21 °C) for 0, 10, 30, 60 and 120 min to replicate how watercress can be treated at home when chopped in salads or other dishes and not consumed immediately after preparation.

Watercress smoothie *(n=3):* 100 g of the plant material was transferred to a juice maker (Vitamix, Total Nutrition Centre, UK), 200 ml of water was added and the watercress was blended for 30 secs at full power. The effect of storage time was also examined by leaving the smoothie on the bench at room temperature (21 °C) for 0, 10, 30, 60 and 120 min.

After processing, all samples were immediately frozen in liquid nitrogen then freeze-dried (Christ A 2-4 LD, Christ, Germany); ground to fine powder using a coffee bean grinder (De'Longhi, Italy), vacuum packed and stored at -20 °C.

Preparation of watercress extracts

Crude methanol (MeOH) extracts: The method used for the preparation of the extracts was adapted from Bell *et al*. [205]. Briefly, 40 mg of ground watercress powder was heated in a dry-block at 75 °C for 2 min to inactivate myrosinase enzyme. Preheated (70 °C) 70% (v/v) MeOH (1 ml) was then added to each sample and placed in a water bath for 20 min at 70 °C. Samples were then centrifuged for 5 min at 6,000 rpm and the supernatant was transferred to fresh tubes. The final volume was adjusted to 1 ml with 70% (v/v) MeOH and stored at -20 °C until the day of analysis. MeOH extracts were used for the FRAP assay, total phenols as well as flavonols and glucosinolates identification and quantification.

Acetone extracts: Total and specific carotenoids were determined in acetone watercress extracts. Watercress powder (25 mg) was weighed out in Falcon tubes (12 ml) previously wrapped in aluminium foil to minimise the degradation of carotenoids by ultra-violet light. Acetone (4 ml) was added to the powder and the samples were shaken for 15 min at 8000 rpm. Following centrifugation at 4000 rpm for 5 min, the supernatant was transferred to a clean tube and the process was repeated (4 ml acetone for the second time and 2 ml the third time) until a colourless supernatant was obtained. The combined supernatants were transferred in fresh tubes and the final volume was adjusted to 10 ml with 100% acetone.

Determination of total phenolics

Total phenols were measured using the method developed by Singleton and Rossi [206] with slight modifications. Briefly, 0.2 ml of the MeOH watercress extract (Section 2.4) or blank was added to 6.0 ml of distilled water in volumetric flasks and mixed with 0.5 ml of Folin - Ciocalteu reagent. A sodium carbonate solution 20% (v/v) (1.5 ml) was added to the mixture and the volume was adjusted to 10 ml. Absorbance was read after incubation of the samples for two hours at room temperature, at 760 nm using a UV-Vis Spectrophotometer (UV-VIS, Perkin Elmers, UK). A standard curve was made using gallic acid in the following concentrations: 0, 50, 100, 150, 250, 500, 750 &1000 mg/L and total phenols were measured as gallic acid equivalents ($R^2 > 0.99$).

Ferric Reducing Antioxidant Power (FRAP) assay

Antioxidant activity of the samples was determined using the FRAP assay based on an adapted version of the method developed by Benzie and Strain [207]. The FRAP reagent was made by mixing 25 ml of 300 mM acetate buffer (pH 3.6), 2.5 ml 10 mM 2,4,6-tripyridyl-s-triazine solution (TPTZ) and 2.5 ml of freshly prepared ferric chloride hexahydrate ($FeCl_3 \cdot 6H2O$). A standard curve was made using L-Ascorbic acid in the following concentrations: 0, 10, 50, 100, 250, 500, 750, 1000 µmol/L ($R^2 > 0.99$). Each sample (MeOH extracts from Section 2.4) or standard (10 µl) was combined with 300 µl of the FRAP reagent and 100 µl of the mixture was transferred in duplicate in a 96-well plate. Absorbance was measured immediately using a plate reader (Tecan GENios, Geneva, Switzerland) at 595 nm.

Total carotenoids

An aliquot of the acetone extracts prepared as previously described (Section 2.4) was used to quantify the total carotenoid content of the samples spectrophotometrically. Absorbance was measured at 470, 645 and 662 nm in a spectrophotometer (UV-VIS, Perkin Elmers, UK). The total amount of carotenoids was calculated according to the following equations by Lichtenthaler [208].

$$C_a = 11.24\, A_{662} - 2.04\, A_{645}$$

$$C_b = 20.13\, A_{645} - 4.19\, A_{662}$$

$$C_{a+b} = 7.05\, A_{662} + 18.09\, A_{645}$$

$$C_{x+c} = \frac{1000\, A_{470} - 190\, C_a - 63.14\, C_b}{214}$$

*Chlorophyll a (C_a), Chlorophyll b (C_b), Total Chlorophylls (C_{a+b}), Total Carotenoids (C_{x+c}). Equations are based on specific absorption coefficients for 100% acetone. The pigment concentrations obtained by inserting the measures absorbance values are µg/ml plant extract solution.

Quantification of carotenoids via HPLC

To determine the amount of lutein, zeaxanthin and β-carotene present, the acetone extracts were used (Section 2.4). Carotenoids were quantified using the method developed by Guiffrida *et al*. [209] with modifications.10 ml of the extract was mixed with 10 ml of diethyl ether, 10 ml of water and 5ml of 10% (v/v) NaCl. Two layers were formed and the lower - acetone phase was discarded. The upper layer containing the ether was collected in a glass vial and anhydrous Na_2SO_4 was added to it to remove any moisture from the solution. The ether phase was transferred to a clean glass vial, the volume was adjusted to 10ml with diethyl

ether and the solution was condensed under nitrogen gas. The dry residue was then reconstituted in 1 ml of methyl tert- butyl ether (MTBE):MeOH (1:1, v/v), filtered using 0.22 µm syringe driven filter unit and analysed by HPLC. The analyses were performed using an YMC30 column (5 µm 250 x 4.6 mm) on a HP Agilent 1050 series HPLC system. The mobile phases used were as follows: Eluent A, consisting of MeOH:MTBE:H_2O (82:16:2 v/v/v) and Eluent B, consisting of MeOH:MTBE:H_2O (23:75:2 v/v/v). The analyses followed a gradient program for the mobile phases, 0 min 0% B, 20 min 0% B, 80 min 70% B, 90 min 70% B. The protocol used a 1 mL/min flow rate and a 100 µL injection volume. UV-vis spectra were gathered in the range of 190-600 nm and the chromatograms were analysed at 450 nm. Identification was based on retention times by comparison with HPLC grade standards of lutein, zeaxanthin and β-carotene (Extrasynthese, France).

Identification and quantification of glucosinolates and flavonols via LC-MS/MS

Methanol extracts, prepared as described above, were used for the quantification of glucosinolates and flavonols in the samples (Section 2.4.1). Each extract (1 ml) was filtered using a 0.22 µm syringe driven filter unit (Millex; EMD Millipore, Billerica, MA, USA) and then diluted using 9ml LC-MS grade water. For the quantification of glucosinolates and flavonols, external calibration curves of 12 mM sinigrin hydrate and isorhamnetin standards were prepared using the following concentrations (56 $ng.\mu l^{-1}$, 42 $ng.\mu l^{-1}$, 28 $ng.\mu l^{-1}$, 14 $ng.\mu l^{-1}$, 5.6 $ng.\mu l^{-1}$, $R^2 > 0.99$). Glucosinolates and flavonols were analysed by LC-MS/MS using an Agilent 1200 LC system coupled to an Agilent 1100 series LC/MS mass trap spectrometer. Separation conditions of samples and MS analysis settings used are identical to those described by Bell, Oruna-Concha [205] . Glucosinolates were quantified at 229 nm and flavonols at 330 nm. The identification was performed using the compounds nominal mass and the analysis of their fragmentation patterns, and also by the comparison with previously published data. All data were analysed using Agilent ChemStation.

Statistical Analysis

The results are presented as the mean of three biological replicates (n = 3) for each sample. One-way ANOVA and Dunnett's multiple comparisons test were used for comparison of all treatments related to the raw watercress. These analyses were carried out using GraphPad Prism version 5.0a for Mac OS X,GraphPad software (Version 5.0a La Jolla, California, USA). Principal component analysis (PCA) and correlation analysis were performed using XL Stat (Version 2016 Addinsoft, New York City, New York, USA).

Results – Part 1

Characterising the metabolic perturbations induced by watercress and phenethyl isothiocyanate exposure in MCF-7 and MCF-10A cells

Aims

- Characterise the basal metabolic profiles of MCF-7 and MCF-10A cells.
- Investigate the metabolic response of MCF-7 and MCF-10A cells in response to crude watercress extract and PEITC.
- Study how crude watercress extract and PEITC influence markers of cellular genotoxicity.

Objectives

- ^{1}H NMR metabonomics and multivariate statistics will be used to characterise the metabolic profiles of the two cell lines following exposure to different doses of the watercress extract and PEITC.
- Treatment genotoxicity will be evaluated by measuring DNA damage using the Comet assay, assessing cell cycle stages using flow cytometry and measuring mitochondrial membrane potential.

Comparative metabonomic profiling of MCF-7 and MCF-10A cells

Metabolic profiles were acquired from the hydrophilic methanol extracts of MCF-7 and MCF-10A cells using ^{1}H NMR spectroscopy. A representative ^{1}H NMR spectrum of cellular metabolites is presented in Fig. 2. Principal components analysis (PCA) was applied to the baseline metabolic profiles of MCF7 and MCF-10A cells to observe the main drivers of variation within the metabolic data. From the scores plot obtained from this PCA model (Figure 3A) clear separation was observed between the two cell lines in the first principal component (PC1). This indicates that the tumorigenic difference of the cell lines is the main source of variation accounting for 22% of the total variation within the data (metabolites). The loadings plot for PC1 from this model (Fig. 3B) indicates that this variation was explained by an increased amount of lactate, phosphocholine and glycine in the MCF-7 cells compared to the MCF-10A.

An orthogonal projection to latent structures discriminant analysis (OPLS-DA) model was built to make a pair-wise comparison between the two cell lines. An OPLS-DA model with strong predictive ability (Q^2Y = 0.5559) was obtained and validated by permutation testing (1000 permutations; p = 0.001). The correlation coefficients plot from this model is presented in Fig. 4. MCF-7 cells contained greater amounts of lactate, the amino acids alanine, glutamine,

glutamate, methionine serine and glycine. MCF-10A cells contained higher amounts of glucose, myo-inositol, choline and creatine phosphate compared to the MCF-7, threonine, as well as choline-related metabolites including phosphocholine and glycine. MCF-10A cells contained higher amounts of glucose, myo-inositol, choline and creatine phosphate compared to the MCF-7 cells.

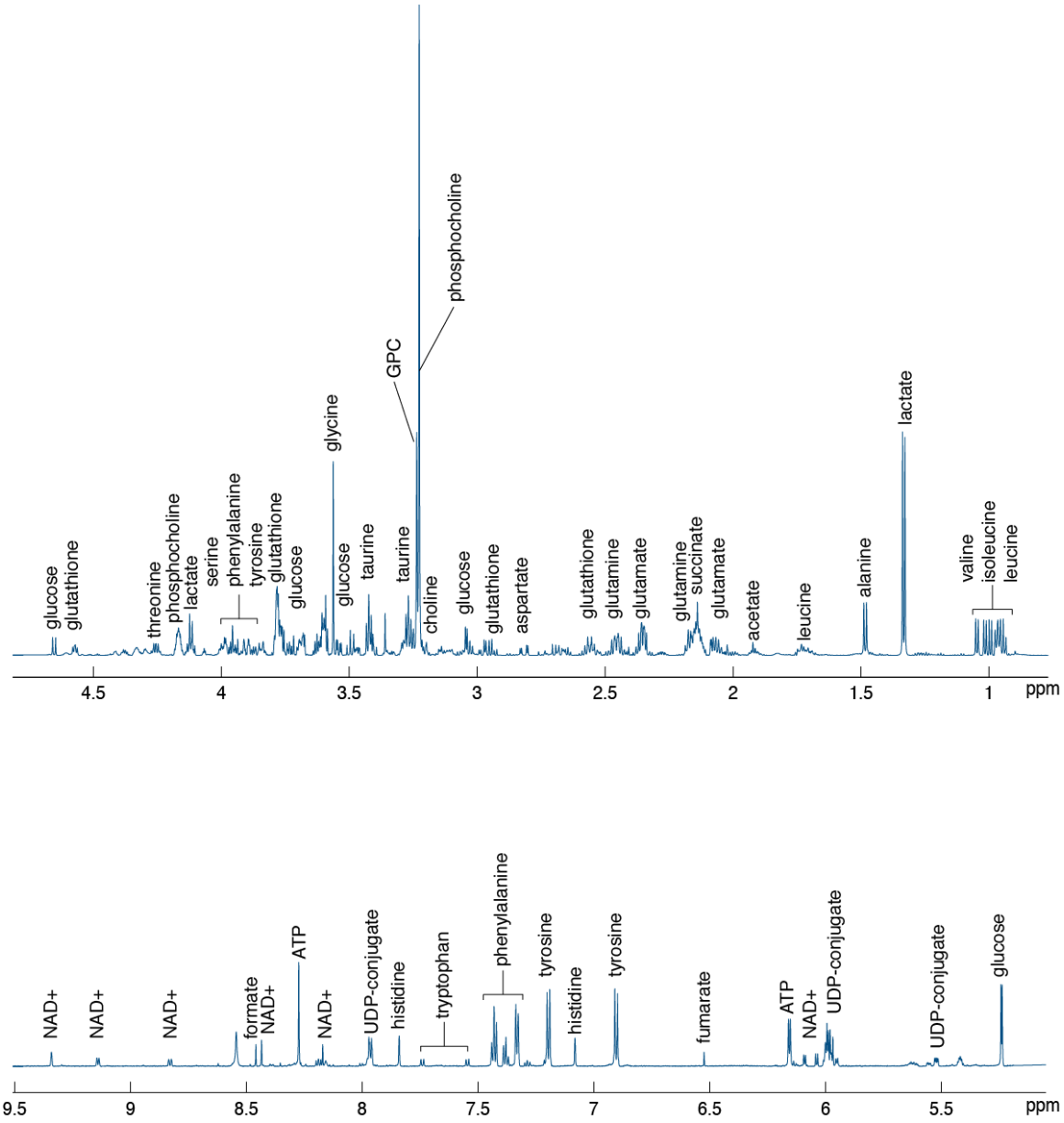

Figure 1 Representative 1H NMR spectrum of the hydrophilic metabolites extracted from untreated MCF-7 cells.

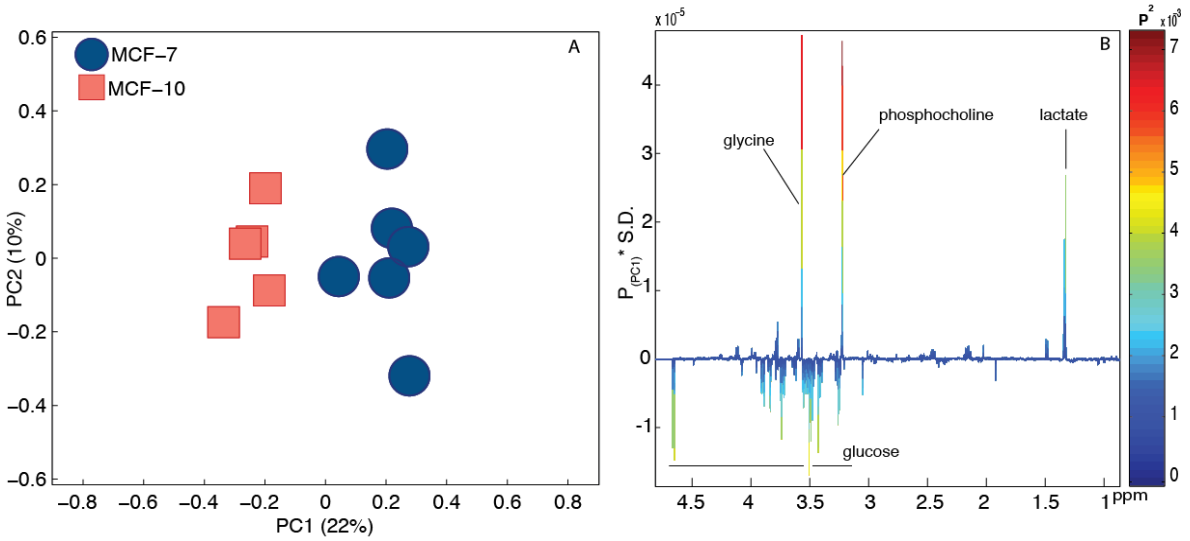

Figure 3 Comparison of the metabolic profile obtained from the two cell lines. (A) PCA scores plot (PC1 vs PC2). (B) PCA loadings plot of PC1.

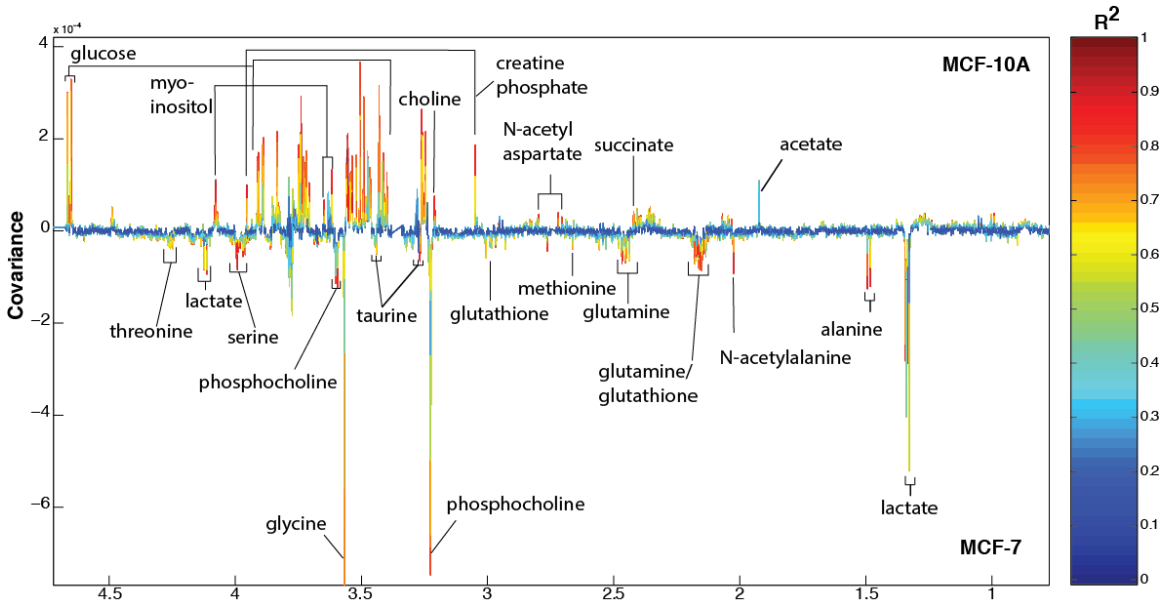

Figure 4 OPLS-DA model identifying metabolic associations with cell type. GPC, glycerophosphocholine

Metabolic profiling with increasing doses of crude watercress extract

MCF-7

PCA was performed on control untreated samples and samples treated with increasing doses of the watercress extract. A clear clustering was observed between the low and the high treatment doses on the first principal component representing 17% of the variation (Fig. 5A). No observable separation was observed between the untreated samples and those treated with the two lower doses (6.25 and 12.5 µl/ml) of the watercress extract. This metabolic transition from low to high doses was explained by increases in the intracellular lactate content of the cells (Fig. 5B). Valid OPLS-DA models with good predictive ability ($Q^2\hat{Y}$) were returned for all the pair-wise comparisons of control MCF-7 cells and cells treated with the different watercress extract doses (Table 1).

Watercress treatment of the MCF-7 cells caused a number of metabolic perturbations including an increase in lactate production at the highest dose (50 µl/ml), elevated amino acid levels (valine, leucine, isoleucine, alanine, asparagine) and also an increase in the glutathione content of these cells. Significant increases of NAD+ were also observed accompanied by increased AXP and essentially a lower ATP content (Fig. 6).

Table 1. Summary of the OPLS-DA models returned for the comparisons between untreated control cells against cells treated with the watercress extract (WX) (6.25 -50 µl/ml) and PEITC (5-30µM) for 24 hours from both MCF-7 and MCF-10A cells.

Treatment	$R^2\hat{Y}$	$Q^2\hat{Y}$	P-value
MCF-7			
Control vs WX 6.25	0.9579	0.4645	0.006
Control vs WX 12.5	0.9871	0.4948	0.002
Control vs WX 25	0.9666	0.7333	0.001
Control vs WX 50	0.9716	0.7525	0.001
Control vs PEITC 5	0.9809	0.4917	0.002
Control vs PEITC 10	0.9884	0.9056	0.002
Control vs PEITC 20	0.9709	0.9317	0.001
Control vs PEITC 30	0.9978	0.9041	0.001
MCF-10A			
Control vs WX 6.25	0.9250	0.4678	0.018
Control vs WX 12.5	0.9344	0.5708	0.004
Control vs WX 25	0.9639	0.7038	0.001
Control vs WX 50	0.9782	0.8248	0.001
Control vs PEITC 5	0.9774	0.0520	0.590
Control vs PEITC 10	0.8776	0.2292	0.250
Control vs PEITC 20	0.9079	0.6422	0.001
Control vs PEITC 30	0.9538	0.8483	0.001

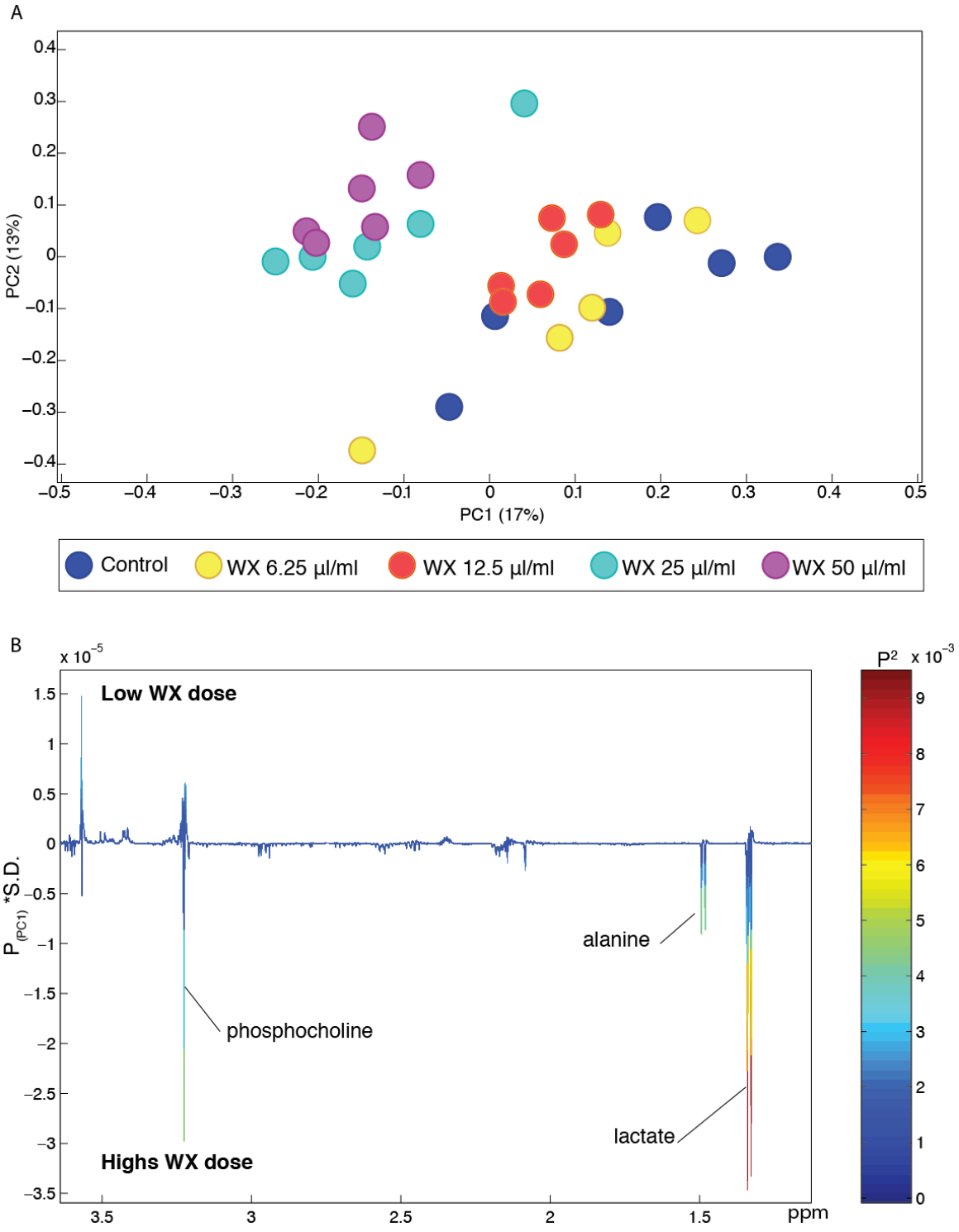

Figure 5. (A) PCA scores plot of the MCF-7 cells treated with increasing concentrations of the watercress extract for 24 hours. (B) PCA loadings plot of PC1

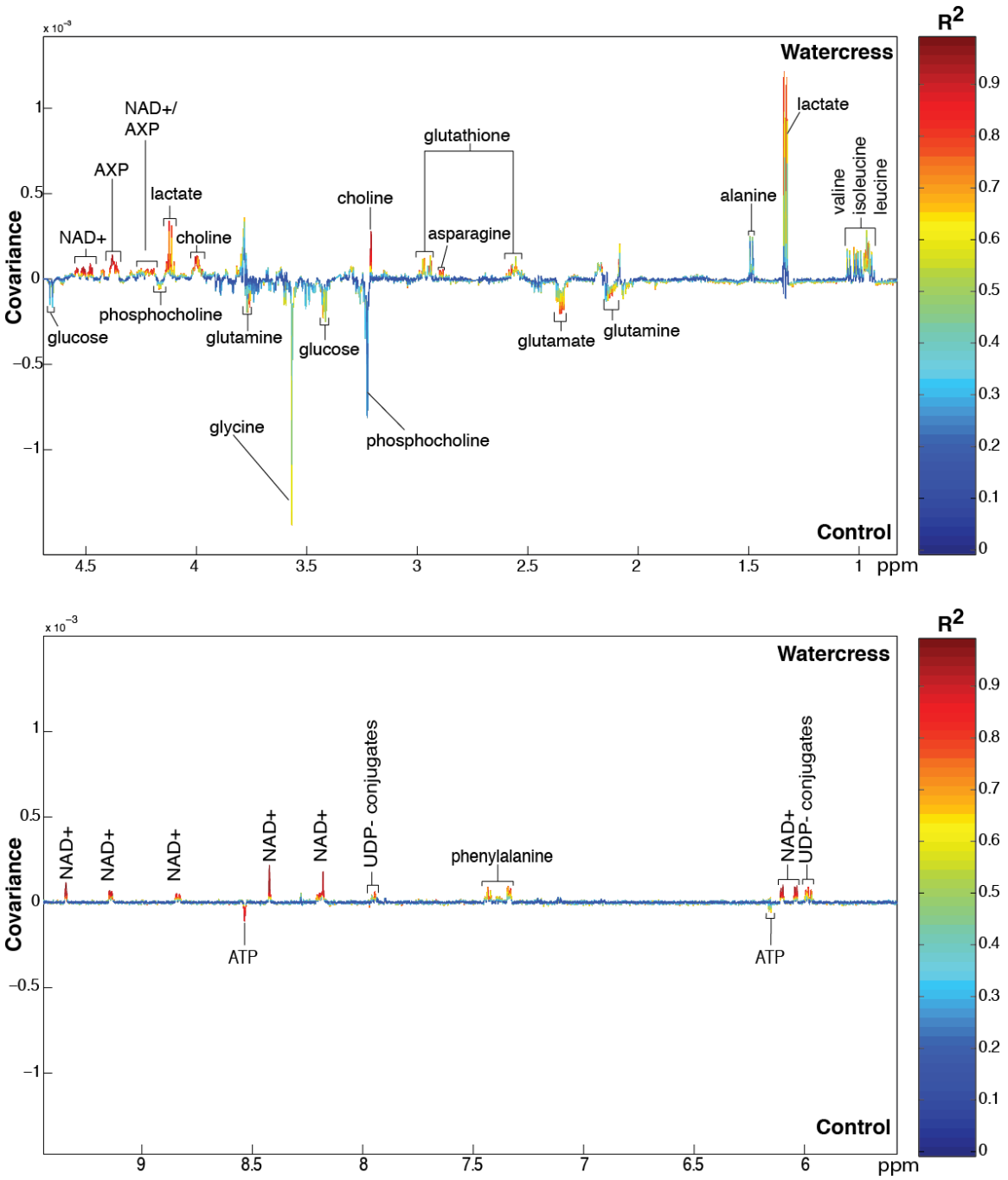

Figure 6. OPLS-DA coefficients plot comparing the metabolic profiles of untreated control MCF-7 cells and WX (50 µl/ml) treated cells. (AXP: indistinguishable difference between AMP and ADP)

MCF-10A

Treatment of MCF-10A cells with the watercress extract caused a metabolic transition from the low to high doses as observed in the PCA scores plot with the different groups separating along PC1 (Fig. 7A). Similarly to the MCF-7 cells, increased lactate explained the variation across the treatment groups (Fig. 7B). An OPLS-DA model was constructed to probe for discriminating features between control and watercress treated cell samples (50 µl/ml). As expected, the model was dominated by elevated lactate in the watercress treated cells with concomitant increases in acetate, succinate and 4-AB as well as choline and glycerophosphocholine. The metabolic profile of the untreated MCF-10A cells contained higher phosphocholine, the amino acids valine, leucine, isoleucine, glutamate, glutamine, methionine and glutathione compared to the watercress treated samples (Fig. 8).

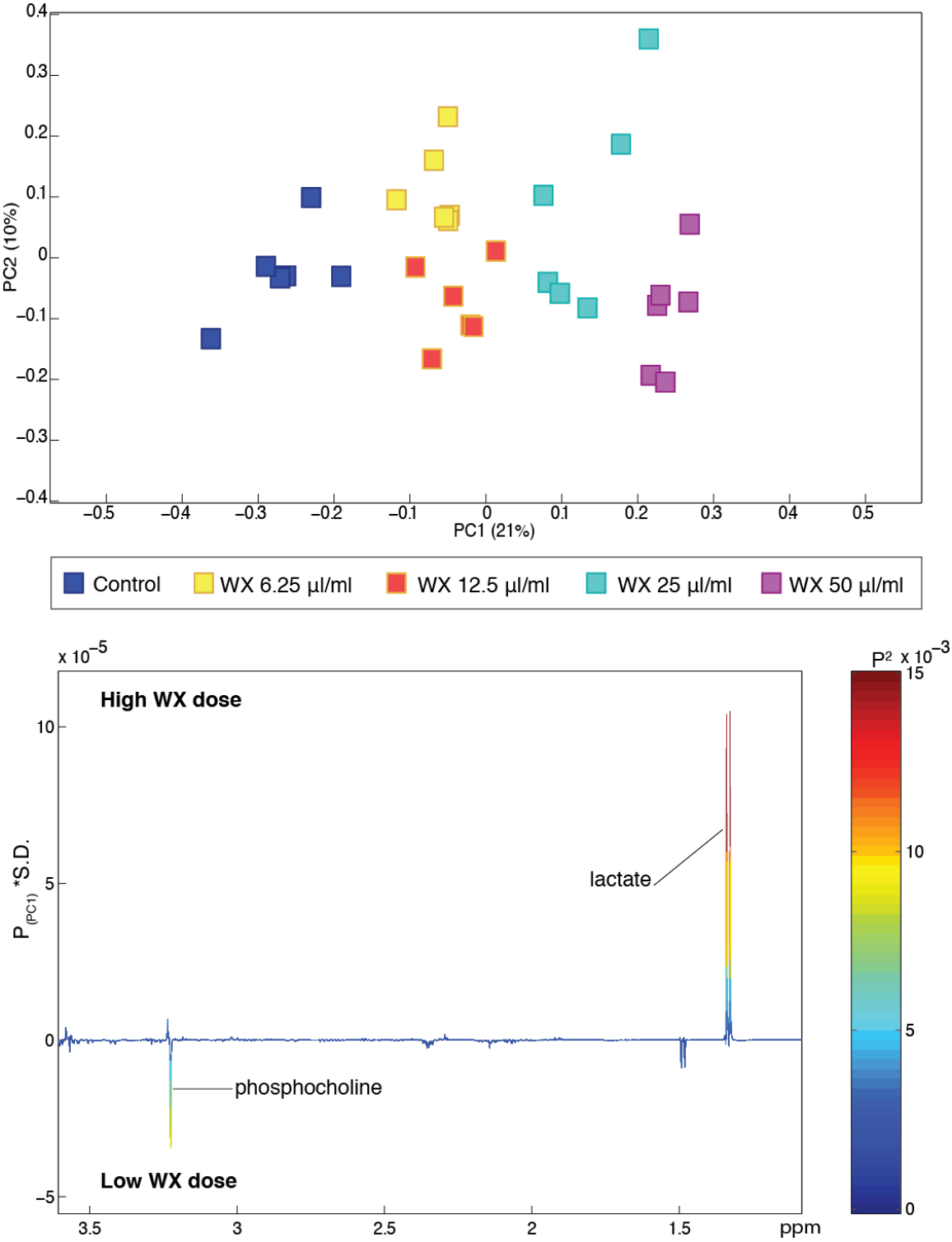

Figure 7. (A) PCA scores plot of the MCF-10A cells treated with increasing concentrations of the watercress extract for 24 hours. (B) PCA loadings plot of PC1

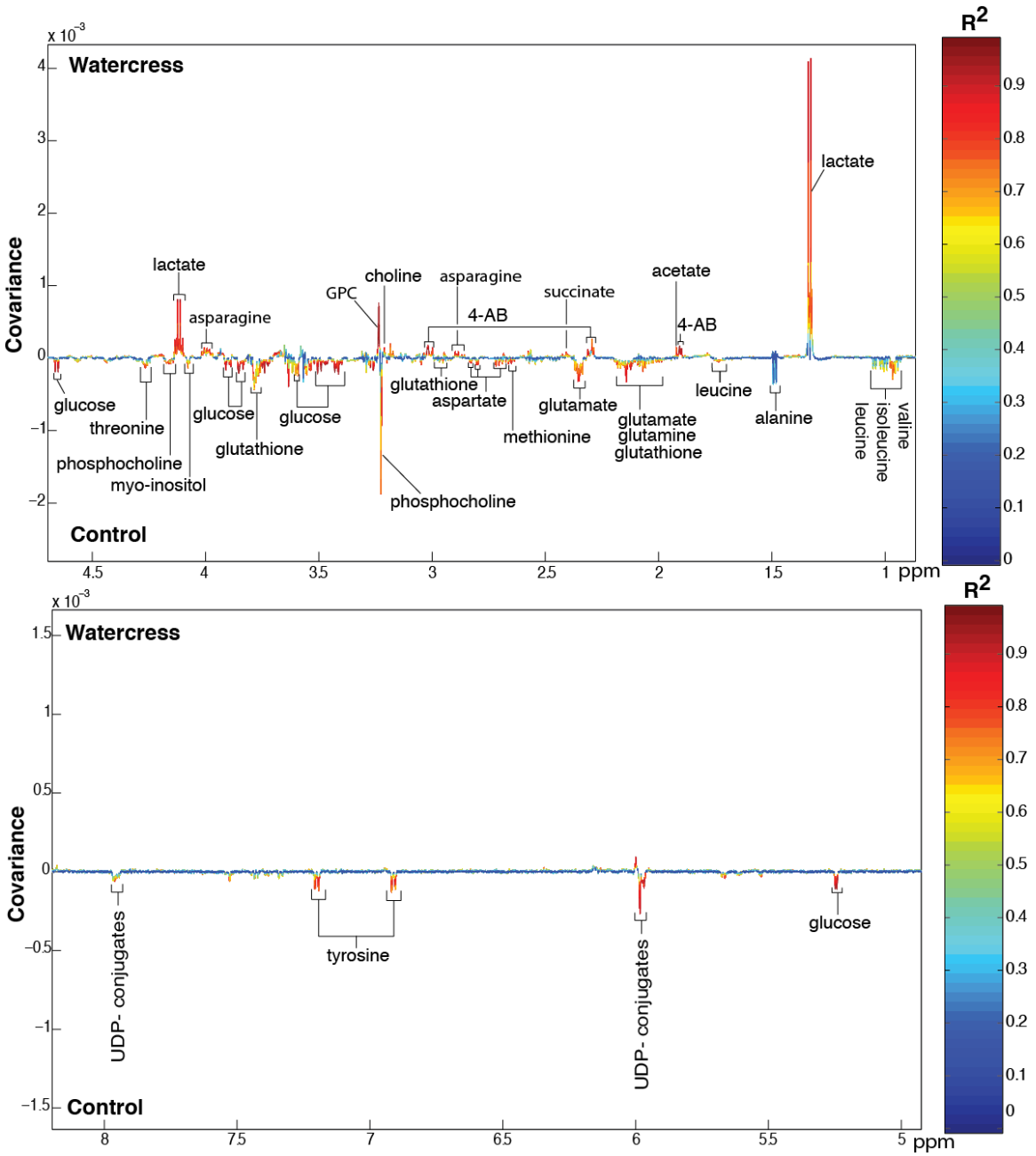

Figure 8. OPLS-DA coefficients plot comparing the metabolic profiles of untreated control MCF-10A cells and WX (50 µl/ml) treated cells. GPC, glycerophosphocholine, 4-AB, 4-aminobutyrate.

Metabolic profiling with increasing doses of PEITC

MCF-7

PCA of control untreated and increasing PEITC dose data from MCF-7 cells revealed two distinct clusters separating on the first principal component representing 42% of the variance in the dataset (Fig. 9A). PCA demonstrated a metabolic trajectory between low and high doses of PEITC driven by lower phosphocholine in the high dose samples compared to the control and low dose samples (Fig. 9B). PCA revealed a metabolic transition between the different doses of PEITC. OPLS-DA models were constructed for a pair-wise evaluation of the effect of the four PEITC dose treatments on MCF-7 cells. Valid models with good predictive ability ($Q^2\hat{Y}$) were returned for the comparisons between control and treated MCF-7 cells (Table 1). PEITC treatment induces strong perturbations in the biochemical signature of these cells and these shifts are dose dependent. Following the high dose exposure to PEITC, lactate, valine, leucine, isoleucine, methionine and threonine, glutamate and glutamine were increased compared to the control and low dose samples. PEITC significantly decreased the amount of choline-related metabolites, phosphocholine and glycerophosphocholine and glycine. MCF-7 cells treated with a high PEITC dose exhibited a characteristic depletion in their glutathione levels and taurine to a lesser extent (Fig. 10). Interestingly, PEITC appears to have a biphasic effect on glutathione, which increases with low PEITC exposure but is depleted with the high dose treatment.

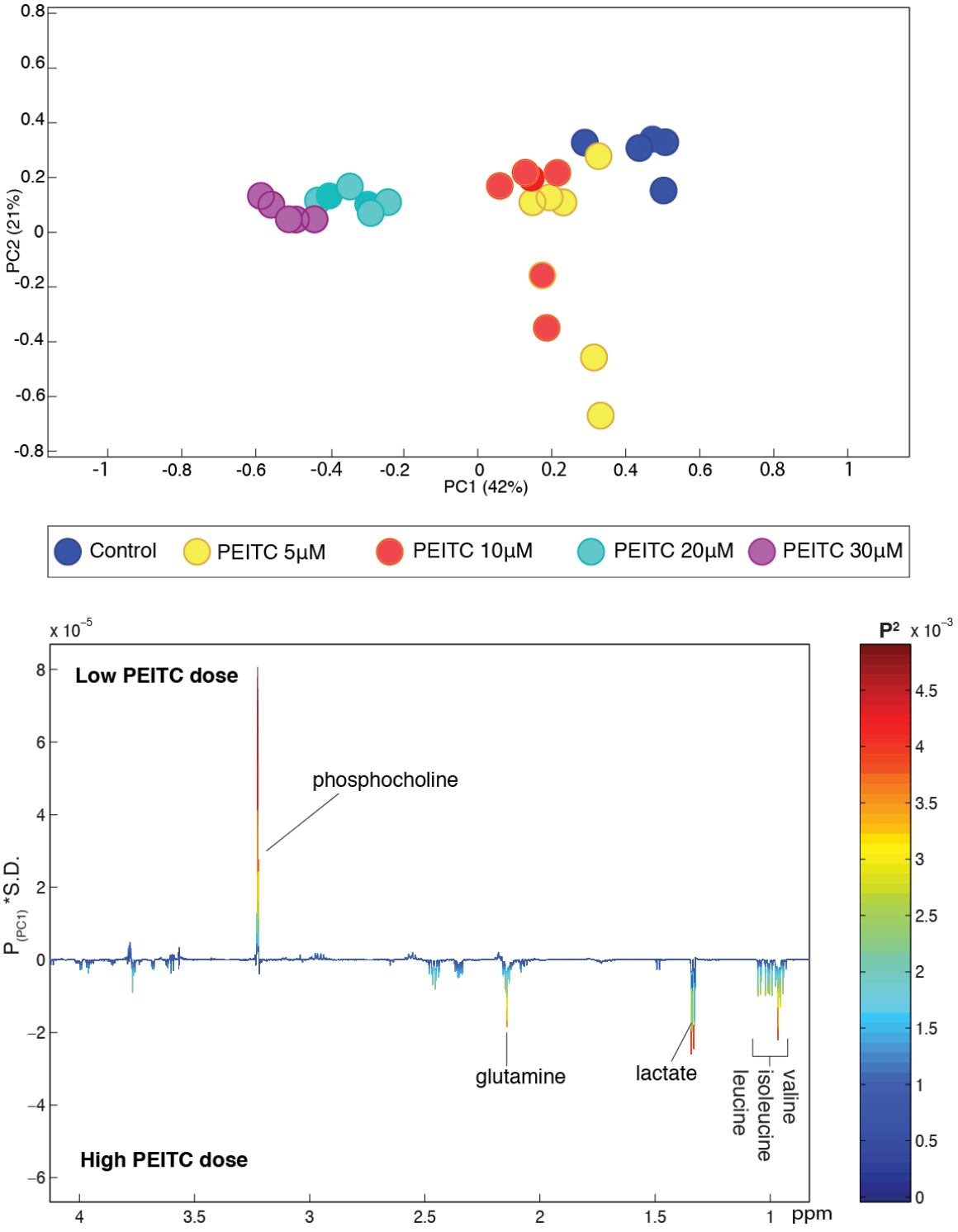

Figure 9. (A) PCA scores plot of the MCF-7 cells treated with increasing concentrations of PEITC for 24 hours. (B) PCA loadings plot of PC1

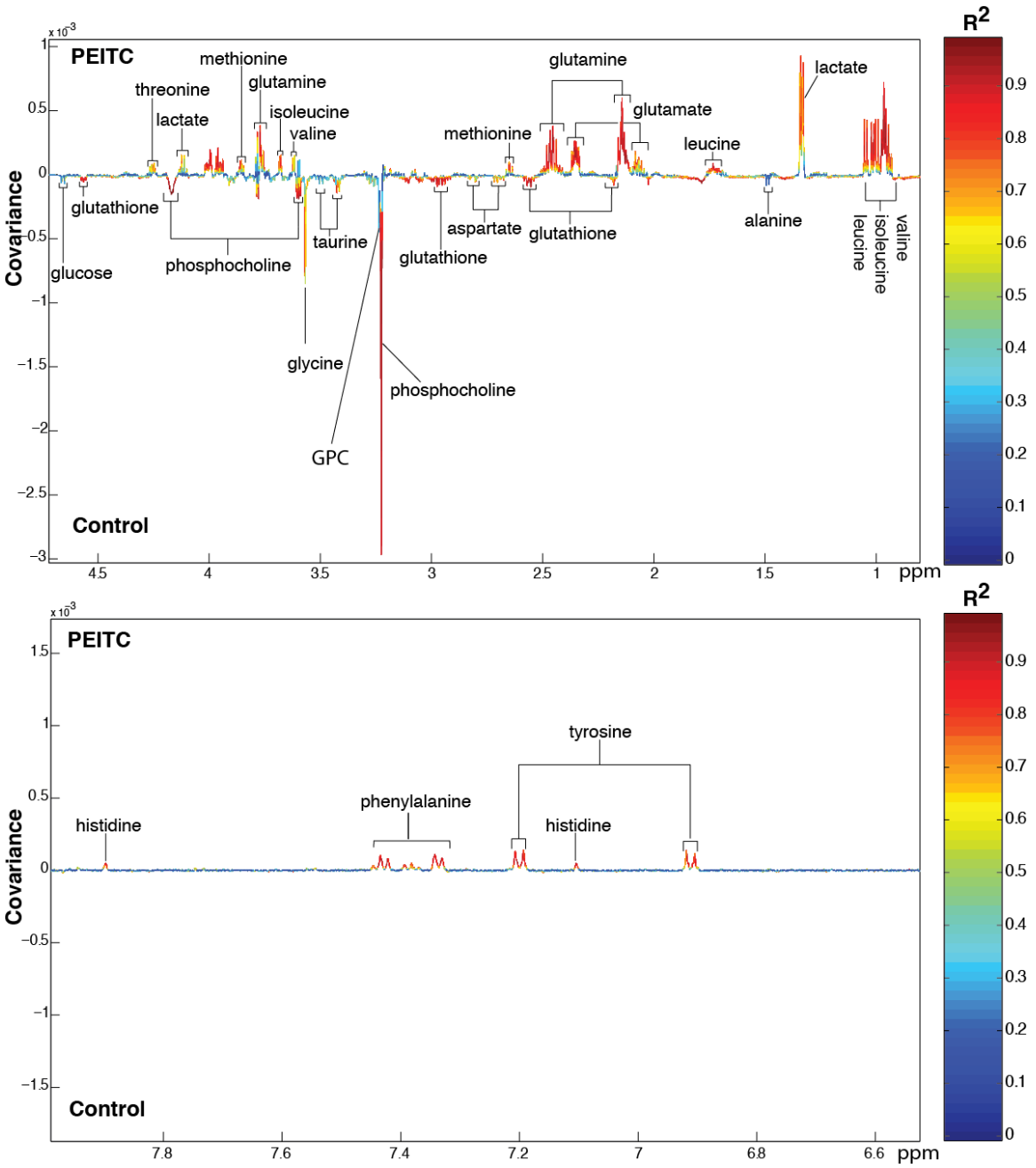

Figure 10. OPLS-DA coefficients plot comparing the metabolic profiles of untreated control MCF-7 cells and PEITC (30 μM) treated cells.

MCF-10A

The metabolic response of MCF-10A cells to PEITC was found to differ compared to that of MCF-7 cells. A dose dependent effect was observed with no discernible differences between control samples and those treated with the 5 or 10 µM of PEITC. Clustering of the cells treated with 30 µM of PEITC was observed on the first principal component (Fig. 11A) and was driven by decreased levels of alanine and phosphocholine in these samples (Fig. 11B).

OPLS-DA models were constructed for a pair-wise evaluation of the effect of the four PEITC dose treatments on MCF-10A cells. The low doses of PEITC (5 and 10 µM) did not have a significant impact on the metabolic profile of the MCF-10A cells. On the contrary, the models built for the pair-wise evaluation of the effects of the two highest PEITC dose treatments were of strong predictive ability (PEITC 20µM, Q^2Y = 0.6422, PEITC 30µM, Q^2Y = 0.8483) and valid upon permutation testing (PEITC 20µM, p = 0.001, PEITC 30µM, p = 0.001). MCF-10A cells responded to PEITC treatment by decreases in their amino acid pool (valine, leucine, isoleucine, threonine, alanine, glutamate, glutamine, methionine), phosphocholine and glycine abundance (Fig. 12). Strikingly, the higher doses of PEITC did not cause depletion in the levels of glutathione or taurine as was the case in the MCF-7 cells, but rather increased their levels.

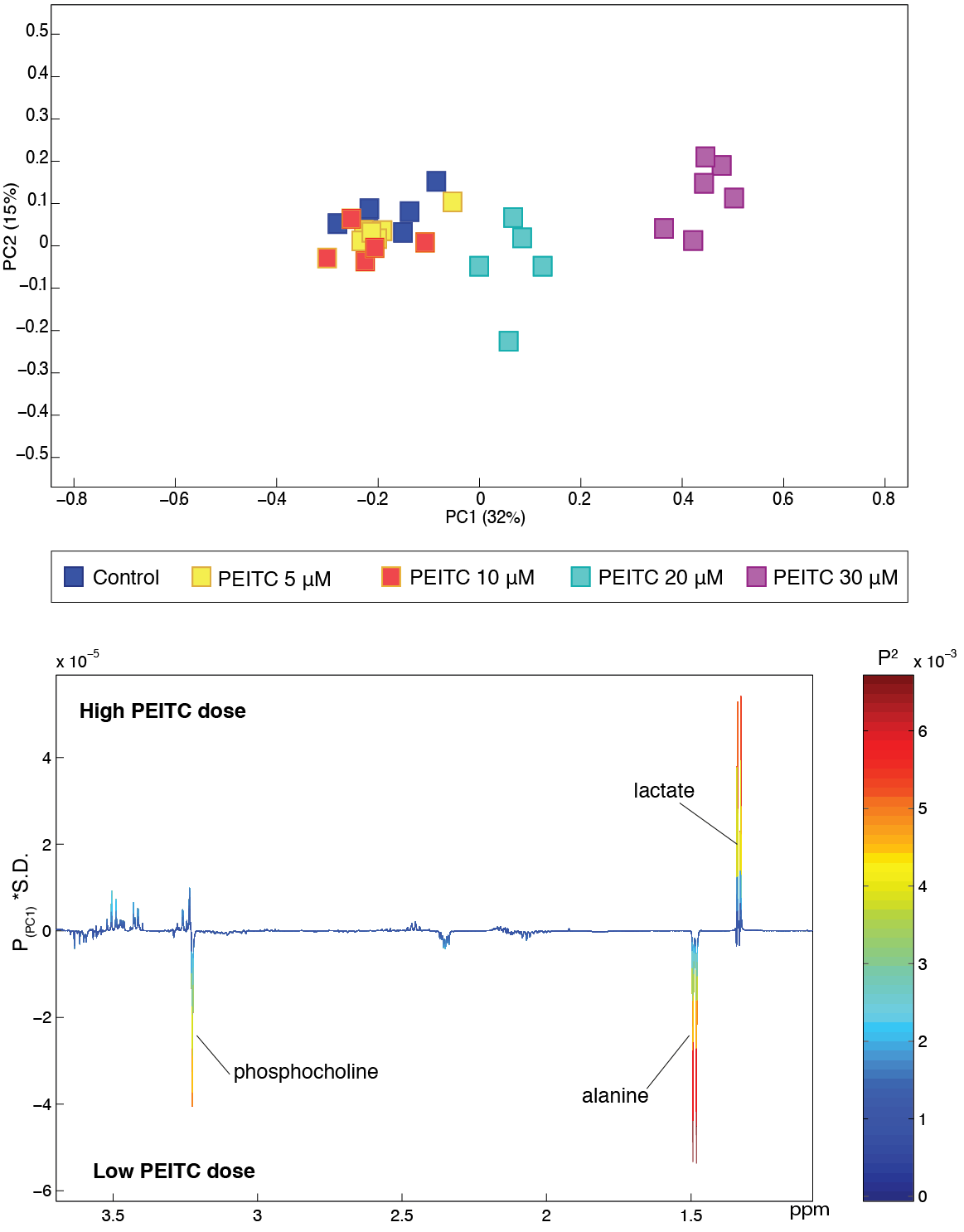

Figure 11. A) PCA scores plot of the MCF-10A cells treated with increasing concentrations of PEITC for 24 hours. (B) PCA loadings plot of PC1

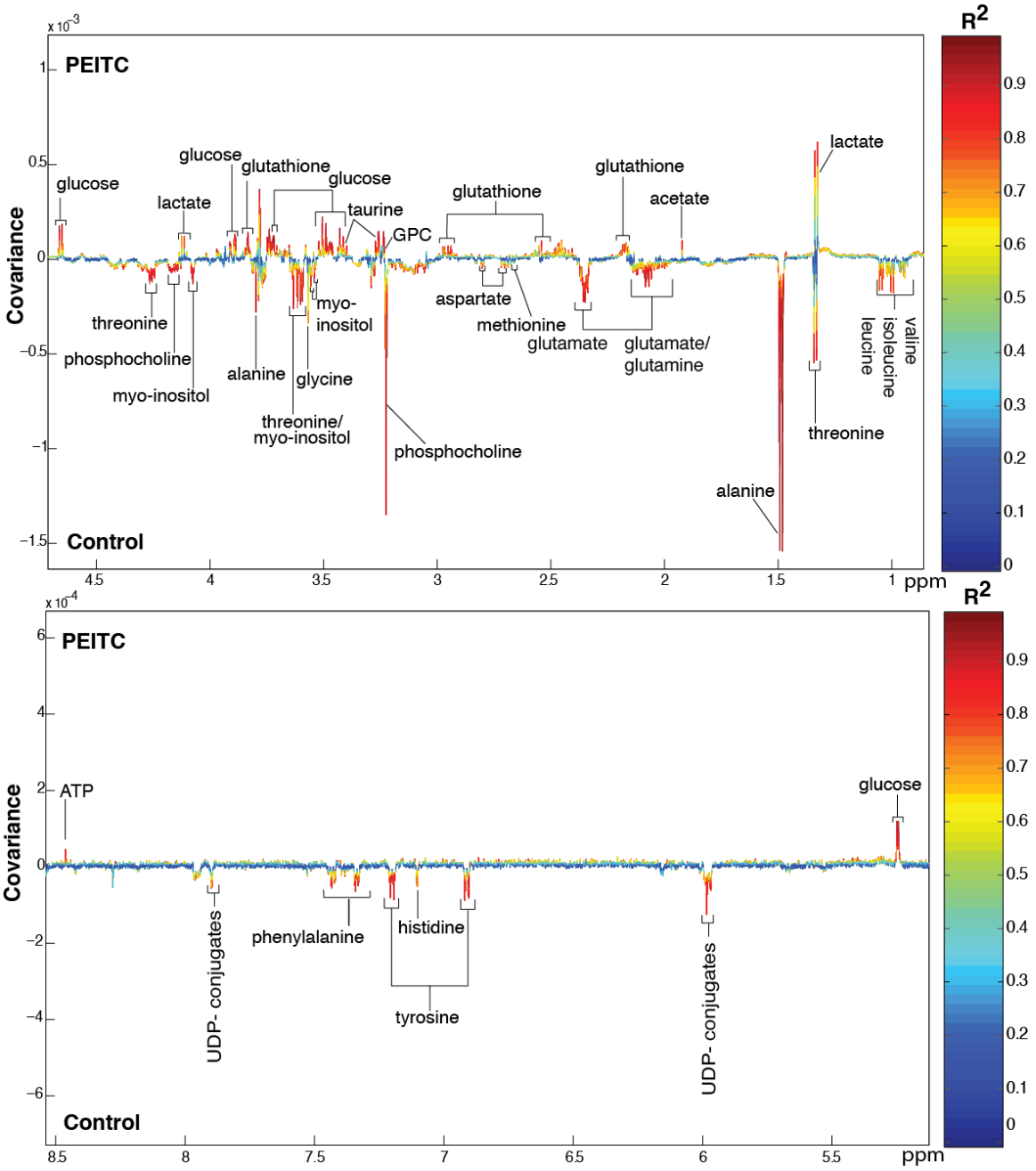

Figure 12. (OPLS-DA coefficients plot comparing the metabolic profiles of untreated control MCF-10A cells and PEITC (30 µM) treated cells.

The metabolic alterations observed from the OPLS-DA models were used to perform unsupervised hierarchical clustering of the metabolites by integrating the corresponding peaks. The results are summarised in Fig 13A and 13 B. A clear metabolic separation of all treatments and doses was observed in the MCF-7 cells but the response of the MCF-10A cells to the different treatments was varied and characterised by some overlap. No observable effects of the low PEITC doses were noted in the MCF-10A cells. MCF-7 cells respond to watercress and PEITC treatments by shifting their metabolic phenotype in an anti-parallel manner. Metabolites like glutathione, aspartate, glycine, phosphocholine and alanine are significantly lower in the MCF-7 cells treated with the higher doses of PEITC but are found in higher levels in the watercress treated cells. In addition, amino acids (threonine, glutamine, methionine, tyrosine, phenylalanine, leucine, isoleucine, valine and histidine) are characteristically elevated in the PEITC treated MCF-7 cells whereas their levels are lower in the watercress treated groups. Comparing the metabolic profiles of the two treated cell lines reveals significant differences in the response of cancer and non-transformed cells upon watercress and PEITC exposure with a more uniform response in the MCF-7 cells.

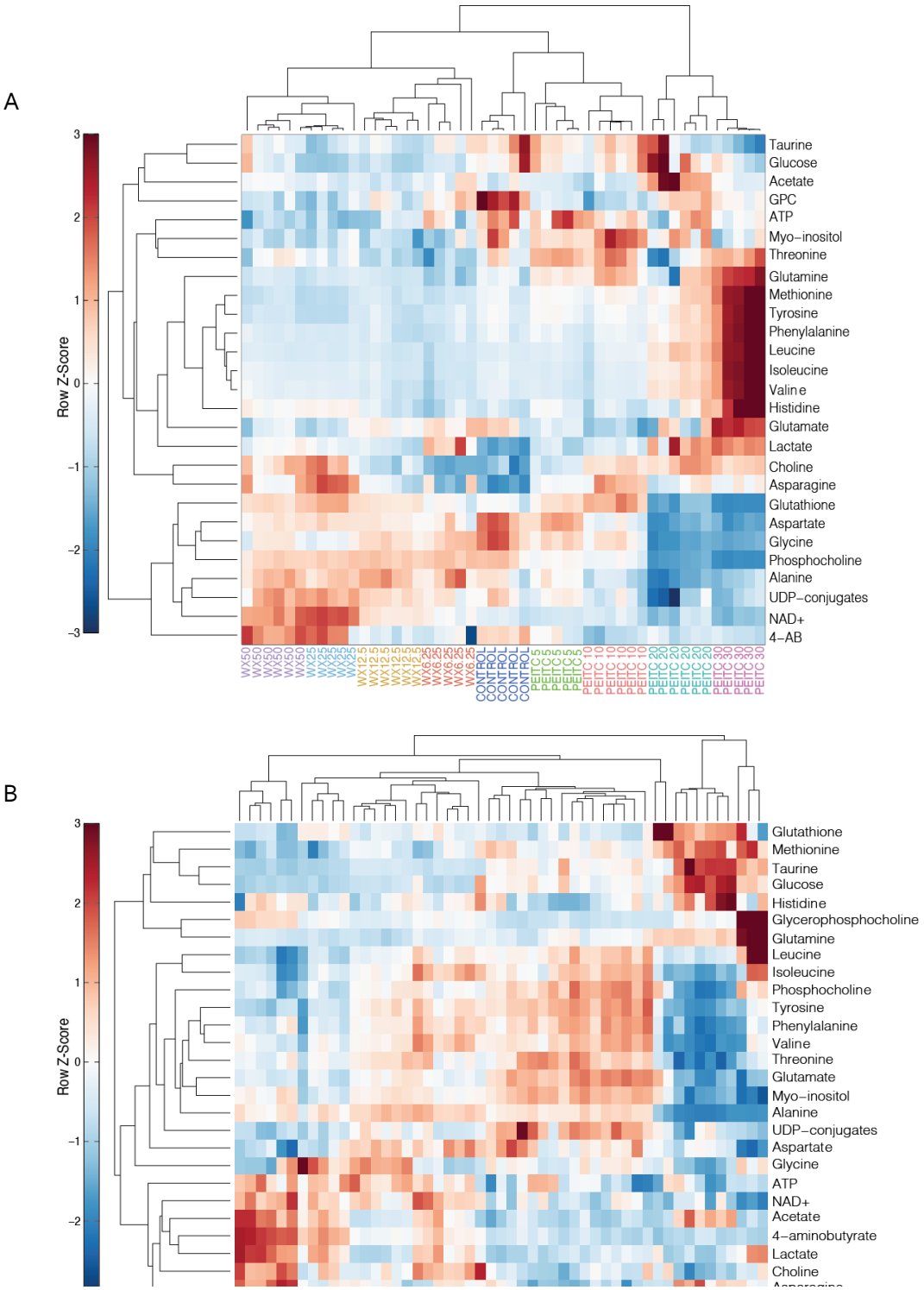

Figure 2. Unsupervised hierarchical clustering heat-map of metabolites from MCF-7 (A) and MCF-10A (B) cells treated with watercress extract or PEITC at increasing concentrations. Each row represents a metabolite and each column represents a sample. The row Z-score (scaled expression value) of each metabolite is plotted in red-blue colour. The red colour indicates metabolites that are high in abundance and blue indicates metabolites low in abundance

Cell Proliferation

Cytotoxicity of increasing doses of the crude watercress extract and PEITC was assessed in MCF-7 and MCF-10A cells. The dose response curves for cytotoxicity as assessed by DAPI staining are presented in Fig. 14 (A-D). Treatment with the watercress extract did not impact MCF-10A proliferation but caused a 20% and 25% decrease in proliferation in MCF-7 cells treated with 25 and 50 µl/ml of the extract, respectively. PEITC caused a significant decrease in cell proliferation in MCF-7 cells reaching up to 46% in the highest PEITC dose (30 µM). Treatment of the MCF-10A cells with 30 µM of PEITC showed evidence of cytotoxicity compared to the untreated control.

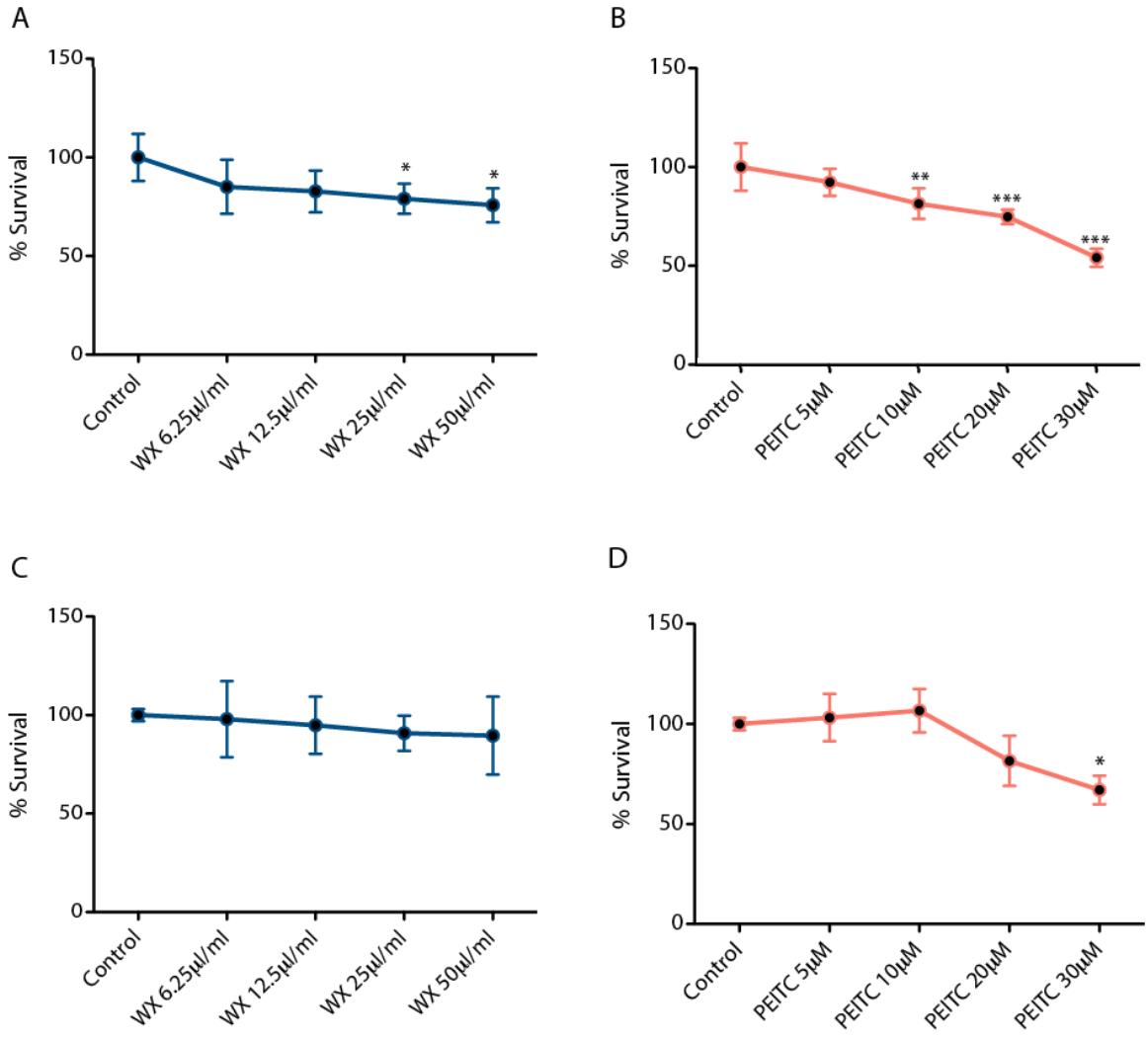

Figure 14. Cytotoxicity of the crude watercress extract and PEITC in MCF-7 (A&B) and MCF-10A (C&D) cells presented as mean ± SEM percentage cell survival. Cells Statistically significant differences between control and treated cells are indicated *p<0.05, **p<0.01, ***p<0.001). Data shown represent the average of three independent experiments with three replicates per sample. WX, watercress.

Cell cycle analysis

Propidium iodide staining was used to assess the impact of watercress extract and PEITC on the cell cycle distribution of MCF-7 and MCF-10A cells.

At the basal level, untreated MCF-7 cells had 10% greater cell distribution in the S phase and 8% in the G2 phase as compared to untreated MCF-10A cells. In MCF-7 cells (Fig. 15) watercress caused a significant 11% reduction in the G1 phase and a parallel increase in the proportion of the cells in the S phase. This effect was dose dependent. PEITC induced a cell cycle arrest at the G1 phase only at the highest doses (20 and 30 µM).

A similar effect of the watercress extract was observed with the MCF-10A cells with an 8% reduction of cells in the G1 phase and a 4% increase of cells in the S phase. In contrast, PEITC did not induce a cell cycle arrest at the G1 stage as observed in the MCF-7 cells. PEITC caused a significant increase in the percentage of cells in the S and G2 phase and a concomitant decrease of the cells in the G1 phase only at the two highest doses.

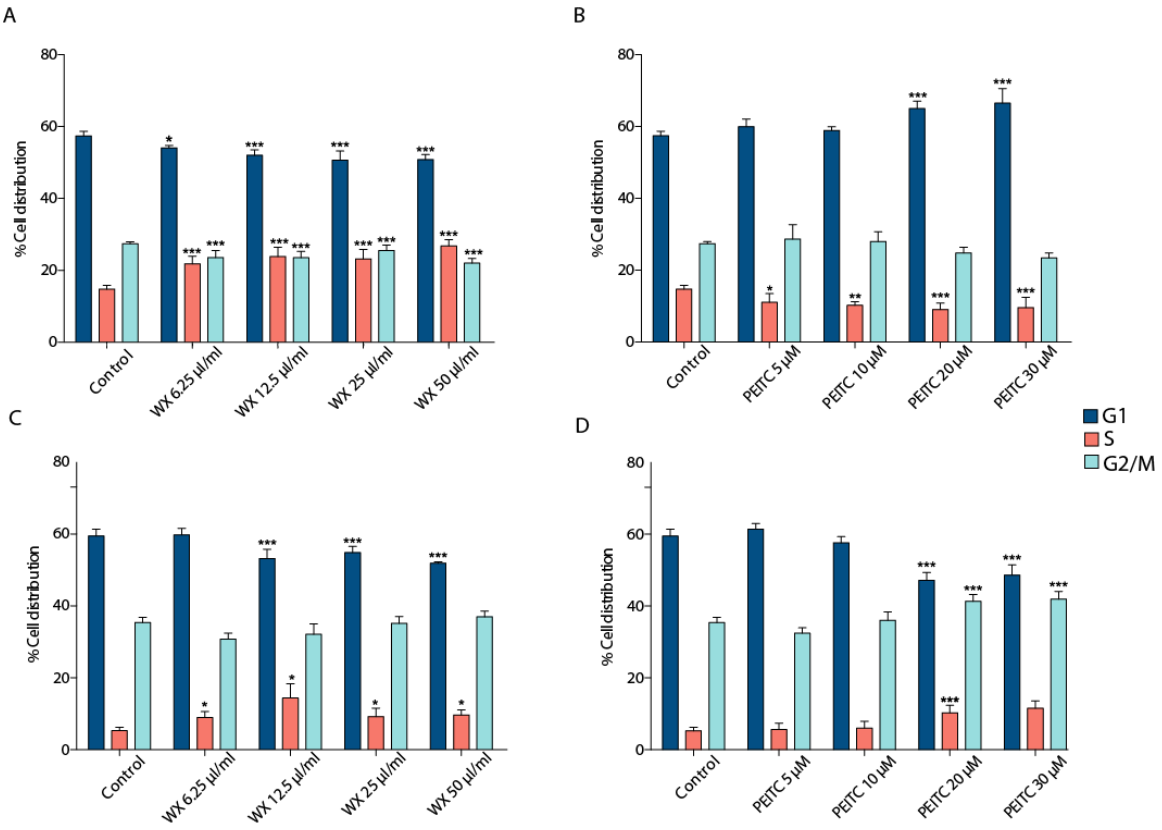

Figure 15. Cell cycle analysis of MCF-7 (A&B) and MCF-10A (C&D) exposed to a range of crude watercress extracts (0-50 µl/ml) and PEITC (0-30µM) for 24 hours. Statistically significant differences between control and treated cells are indicated *p<0.05, ***p<0.001). Data shown represent the average of three independent experiments + SEM with two replicates per sample. WX, watercress.

DNA oxidative damage

MCF-10A cells appeared to have slightly lower basal DNA damage (8.8 ± 1.4%) as compared to MCF-7 cells (13.6 ± 1.6%) (Fig.16). Crude watercress extract did not appear to induce any significant genotoxic effects in either cell line at any of the concentrations tested. PEITC on the other hand was genotoxic in both cell lines at 20 and 30 µM with significantly increased % tail DNA. In MCF-7 cells PEITC 20 µM and 30 µM caused 14.1% and 19.2% additional damage respectively. In MCF-10A cells the same treatments induced a further 4.7% and 8.2% damage respectively.

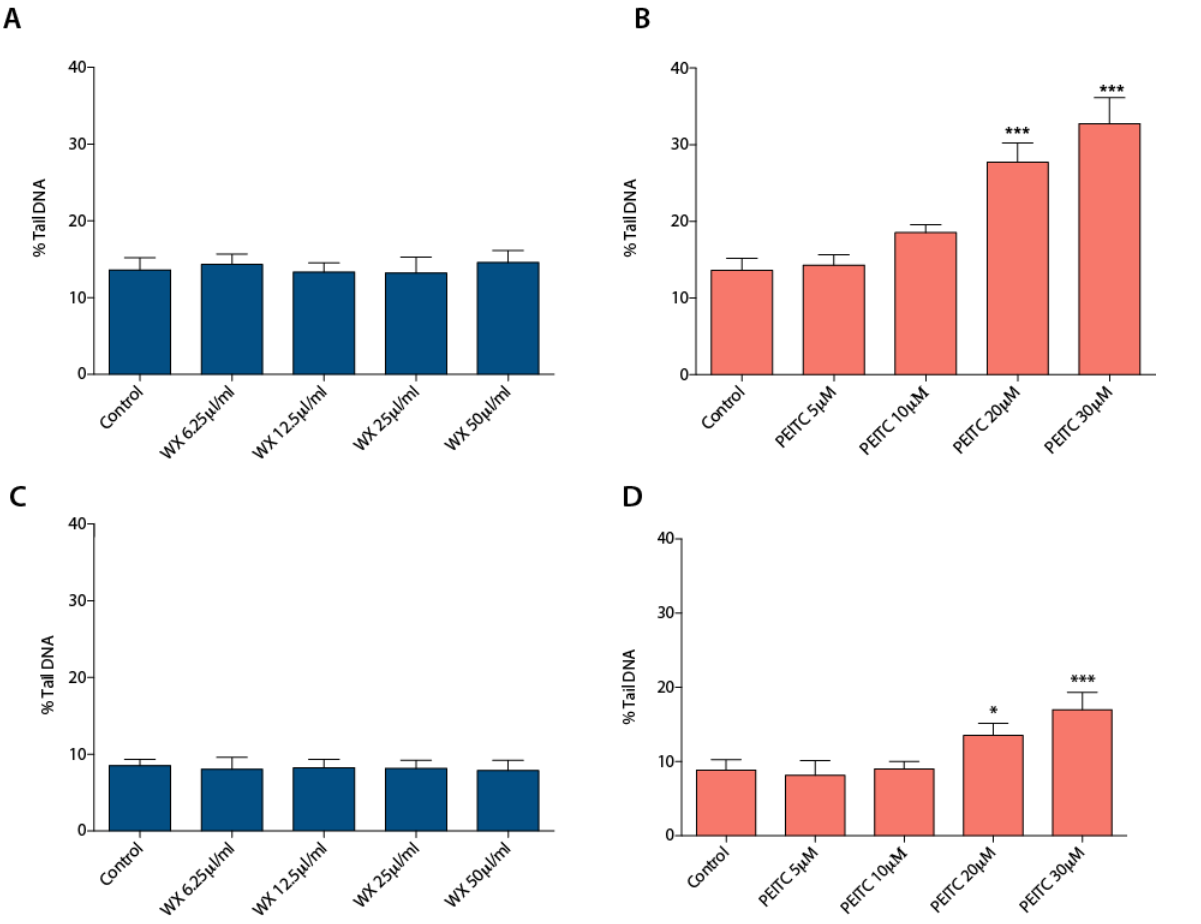

Figure 16. Genotoxic effects of the crude watercress extract and PEITC on MCF-7 (A&B) and MCF-10A (C&D) cells after a 24-hour incubation. Statistically significant differences between control and treated cells are indicated *p<0.05, ***p<0.001). Data shown represent the average of three independent experiments + SEM with two replicates per sample. WX, watercress.

Mitochondrial membrane potential

The impact of increasing doses of the crude watercress extract and PEITC on the mitochondrial membrane potential was assessed by fluorescent JC-10. Crude watercress extract did not affect the membrane potential of MCF-10A cells but induced significant increase in the polarisation of the mitochondrial membrane of MCF-7 cells (Fig.17). A remarkable loss of mitochondrial membrane potential was observed in the PEITC treated groups with the polarisation increasing by 148% in the highest PEITC dose in MCF-7 cells. MCF-10A cells were more resistant to the lower doses of PEITC but showed 65% and 115% increase in polarisation in the two high PEITC doses respectively.

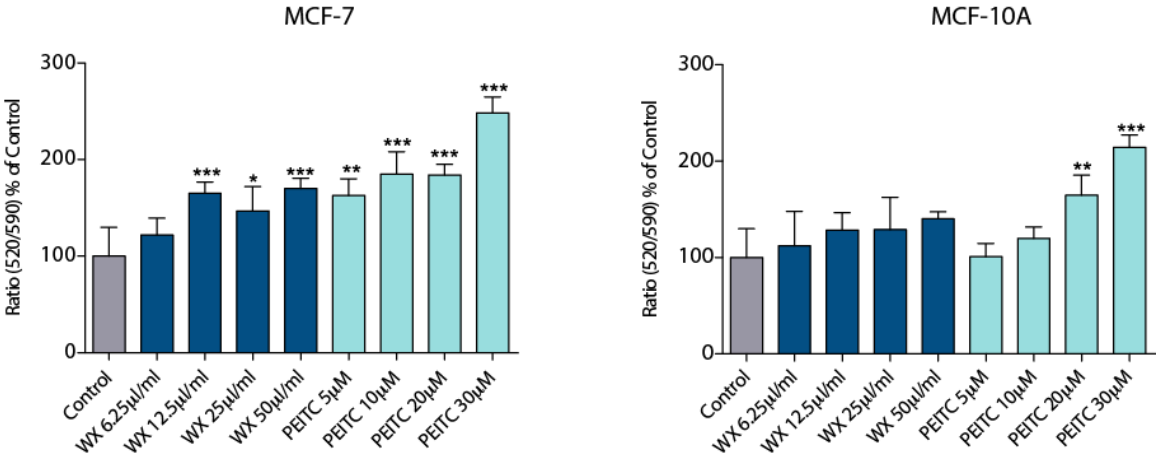

Figure 17. Impact of PEITC and the crude watercress extract on the mitochondrial membrane potential of MCF-7 and MCF-10A cells as evaluated by increased JC-10 monomer/aggregate ratio (520/590 nm). Statistically significant differences between control and treated cells are indicated *p<0.05, ***p<0.001). Data shown represent the average of three independent experiments + SEM with three replicates per sample. WX, watercress.

Part 1 – Main findings

- Watercress and PEITC compromised the viability of cancer cells. Watercress extract did not affect the viability of healthy cells but PEITC was toxic to them
- PEITC caused significant DNA damage to both cell lines whereas watercress did not appear to be genotoxic.
- DNA damage by PEITC resulted in cell cycle arrest in cancer cells and substantial damage to the mitochondrial membranes
- PEITC and watercress interacted with the metabolic landscape of both cell lines. PEITC depleted cancer cells of glutathione, which could render them more susceptible to damaging agents.

Results – Part 2

Sensitisation of human breast cell lines to ionising radiation by phenethyl isothiocyanate and watercress extract

Hypothesis

We hypothesise that phenethyl isothiocyanate (PEITC) sensitises cancer (MCF-7) cells, but not healthy (MCF-10A) cells, to ionising radiation (IR) and that watercress extract protects healthy cells from IR induced collateral damage while enhancing the deleterious effects of IR in cancer cells.

Aims

- Examine the combined effect of PEITC or watercress pre-treatment with IR on physiological parameters of cell function and genotoxicity
- Characterise the metabolic response of MCF-7 and MCF-10A cell lines to IR.
- Investigate how the metabolic profile of the MCF-7 and MCF-10A cells is affected by a pre-treatment with PEITC or with watercress extract prior to IR exposure

Objectives

- Expose MCF-7 and MCF-10A cells to X-ray IR and measure DNA damage using the Comet assay and cell cycle progression using flow cytometry.
- Define the metabolic variation between cell type, PEITC or watercress pre-treatment and IR using ^{1}H NMR metabonomics and multivariate statistics

Cell viability

The impact of combined IR and PEITC or watercress treatment on cell survival was assessed using the MTT assay (Fig 18). At a dose of 5 Gy, IR decreased mean cell survival in both cell lines, although not reaching statistical significance ($p>0.05$). Significant decreases in the survival of both cell lines were observed with PEITC pre-treatment prior to IR. Cell viability was decreased by 86 % in MCF-7 cells exposed to 20 μM of PEITC ($p<0.01$) and 66 % in MCF-10A ($p<0.05$) relative to IR alone. Exposure to the watercress prior to IR did not have an impact on cell viability in either MCF-7 or MFC-10 cells compared to irradiated cells. Combined exposure to both doses of watercress and IR resulted in significant decrease in cell viability when compared to the non-irradiated controls ($p<0.01$; Fig 18).

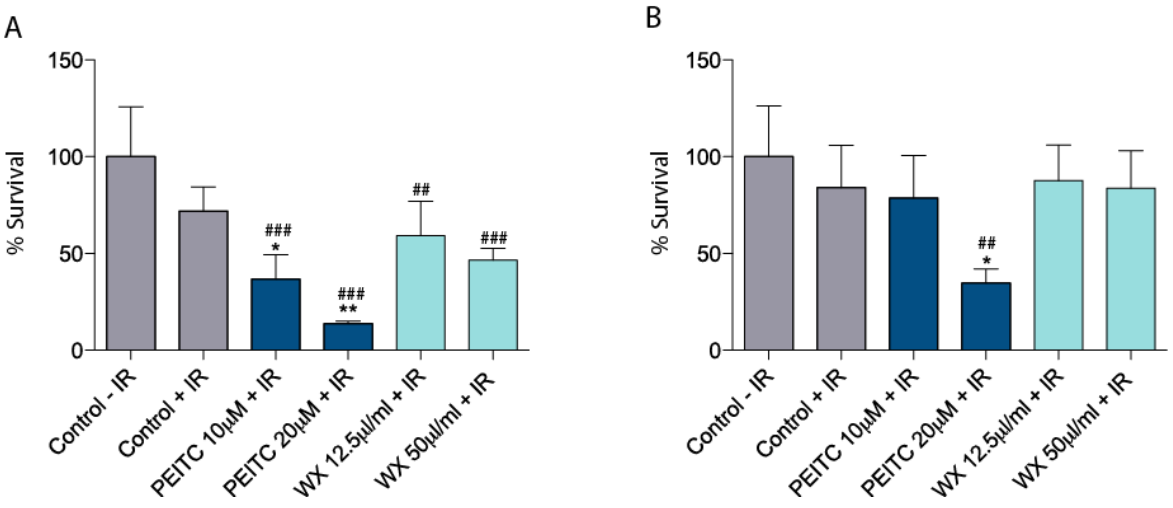

Figure 18. Effect of PEITC and watercress extract (WX) pretreatment (24 hours) combined with 5 Gy of IR on MCF-7 (A) and MCF-10A (B) cell viability. Statistically significant differences between groups are indicated as follows: ##$p<0.01$, ###$p<0.01$, for comparisons to 'Control – IR' *$p<0.05$, **$p<0.01$ for comparisons to 'Control+IR'. Data shown represent the average of three independent experiments + SEM with three replicates per sample.

Cell cycle analysis

Cell cycle kinetics were assessed using propidium iodide staining; the MCF-7 cultures had a much higher number of cells in S-phase than was observed with the MCF-10A cells, this is consistent with a higher proliferative capacity for the cancer cell line. The response to a 5 Gy IR dose also differed; in the MCF-7 cells there was an accumulation of cells in G2 arrest coupled to a decrease in the number of cells in S phase (Fig 19). In contrast the MCF-10A cells responded to IR by increasing the proportion of cells in the G1 phase of the cell cycle (~6%) (Fig. 19B) coupled to an 11% reduction in the percentage of cells in G2.

Pre-treatment of MCF-7 and MCF-10A cells with the watercress extract or with PEITC differentially sensitised cells to a subsequent dose of 5 Gy IR, (Fig. 19A and B). In the MCF-7 cells pre-treatment with PEITC (20 μM) led to a further reduction in the number of irradiated cells in S-phase, and an accumulation of irradiated cells in G1 cell cycle arrest with a reduction in the proportion of cells in G2 relative to non-pretreated irradiated controls. The same dose of PEITC alone caused a 7.6% increase in the proportion of the cells in G1 phase but when combined with IR the proportion increased to 18.4% (Fig. 19C). In the MCF-10A cells, PEITC caused a minor decrease in the proportion of the cells on the G2 phase coupled to an increase in the percentage of the cells in the S phase (Fig 19).

In contrast to PEITC, watercress increased the percentage of IR cells in S phase in both cell lines. In the MCF-7 cells this was coupled to a decrease in the proportion of cells in G2, whereas in the MCF-10A cells the proportion of cells in G1. These observations were not observed in non-irradiated watercress treated cells.

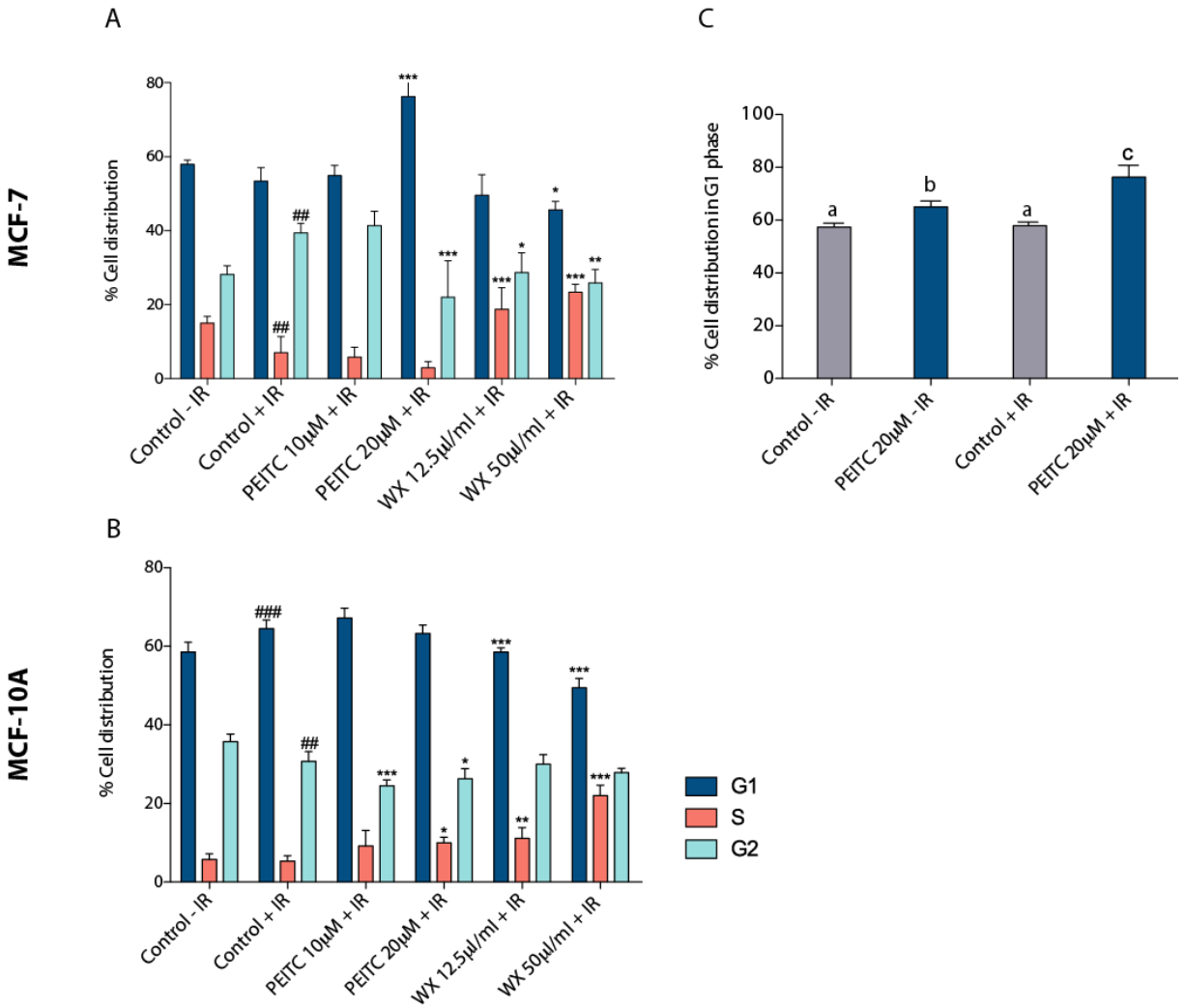

Figure 19. Cell cycle analysis of MCF-7 (A) and MCF-10A (B) cells exposed to 5 Gy of IR following a 24 hour pre-treatment with PEITC or crude watercress extract (WX). Statistically significant differences between irradiated control and treated cells are indicated *p<0.05, **p<0.01, ***p<0.001 and significant differences between non-irradiated and irradiated cells are indicated ##p<0.01, ### p<0.001. (C) % Distribution of MCF-7 cells in G1 upon treatment with PEITC or IR. Different letters suggest statistical significance (p<0.05). Data shown represent the average of three independent experiments + SEM with two replicates per sample.

DNA oxidative damage

To further assess if the observed cell cycle arrest was a response to DNA damage, MCF-7 and MCF-10A cells were treated with PEITC and the crude watercress extract for 24 hours followed by exposure to 5 Gy of IR and DNA lesions were quantified using the Comet assay. IR induced a 39 % increase in tail DNA in MCF-7 cells and pre-treatment with 20 µM of PEITC significantly increased the damage by a further 15 % resulting in a final 66% tail DNA content (Fig. 20). Exposure of the MCF-7 cells to 50 µl/ml of the watercress extract also increased DNA damage levels by 7% compared to the irradiated but non-treated control cells.

MCF-10A cells exhibited sensitivity to IR but to a much lesser extent than the cancerous cells. Tail DNA content in IR- exposed cells was 19% compared to 8% in control, untreated cells. However 24 hour pretreatment with 10 µM of PEITC and 50 µl/ml of watercress extract significantly reduced the comet tail DNA from 19.37% in the irradiated cells to 14% and 10.5% respectively. The highest dose of PEITC combined with 5 Gy of IR was genotoxic to the non-tumorigenic cells resulting in a final 44 % tail DNA.

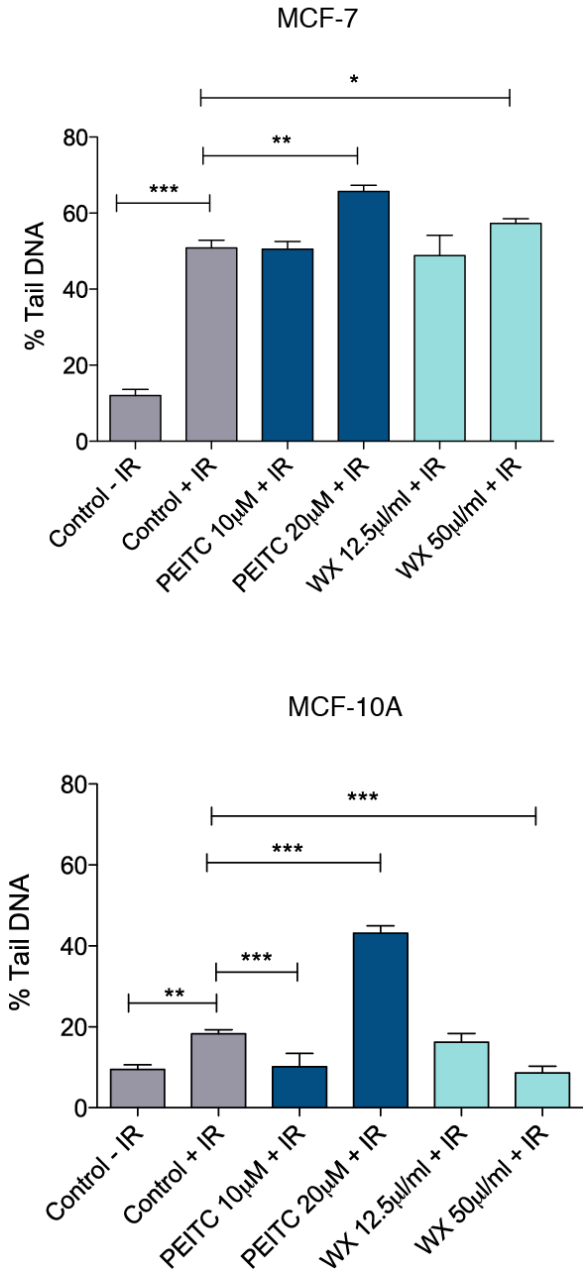

Figure 20. DNA damage levels in MCF-7 and MCF-10A cells exposed to 5 Gy of IR following 24 hour pre-treatment with PEITC or crude watercress extract (WX). Statistically significant differences between groups are indicated as follows *p<0.05, **p<0.01, ***p<0.001. Data shown represent the average of three independent experiments + SEM with two replicates per sample.

Metabonomic profiling of MCF-7 and MCF-10A cells in response to IR exposure

MCF-7

Metabolic profiles were obtained from the cell extracts of MCF-7 cells exposed to 5 Gy IR and of untreated control cells. Principal component analysis (PCA) was applied to these profiles to reveal the main source of variation within the metabolic data. The scores plot obtained from the PCA model (Fig. 21A) showed a separation along the first principal component, indicating that IR exposure accounts for 25% of metabolic variation. The loadings plot for PC1 from this model (Fig. 21B) shows that phosphocholine and glycine explained the variation in the model, both being present in higher amounts in the non-irradiated MCF-7 cells.

An orthogonal projections to latent structures discriminant analysis (OPLS-DA) model was constructed to perform a pair-wise comparison between the untreated and irradiated cells (Fig. 22). A valid OPLS-DA model with good predictive ability ($Q^2\hat{Y}$=0.462) was obtained and validated by permutation testing (1000 permutations; *p*=0.005). The metabolites associated with IR in MCF-7 cells are shown in the coefficients plot extracted from the OPLS-DA model. Irradiated MCF-7 cells contained lower amounts of glutathione and phosphocholine as well as glutamine and glutamate, but had higher amounts of lactate, taurine and glucose compared to the non-irradiated cells.

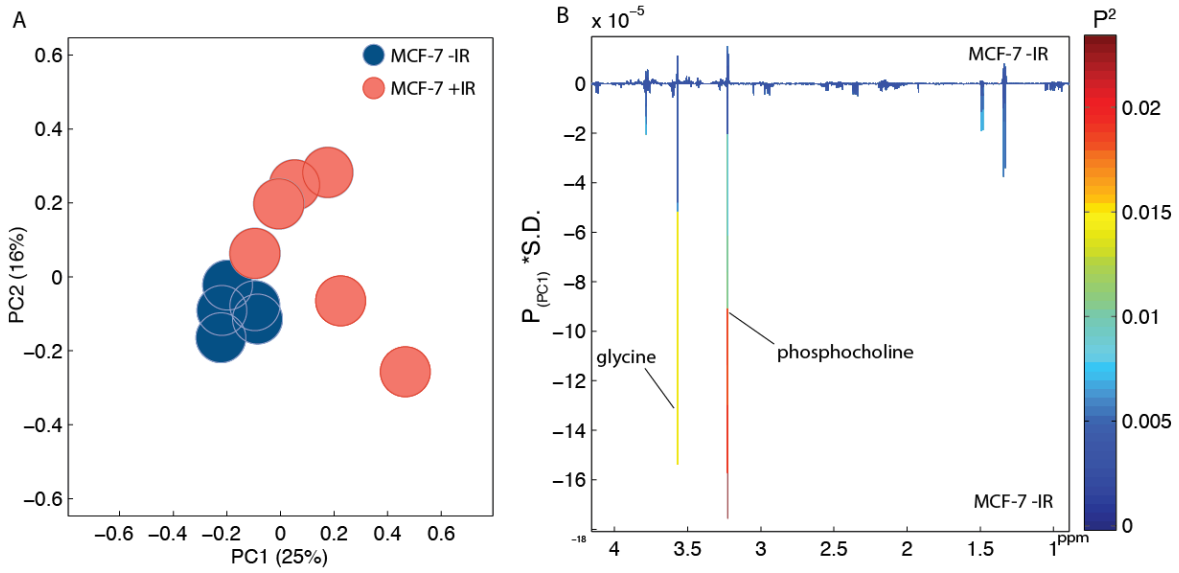

Figure 21. (A) PCA scores plot of MCF-7 untreated cells and cells exposed to 5 Gy IR. (B) PCA loadings plot for PC1.

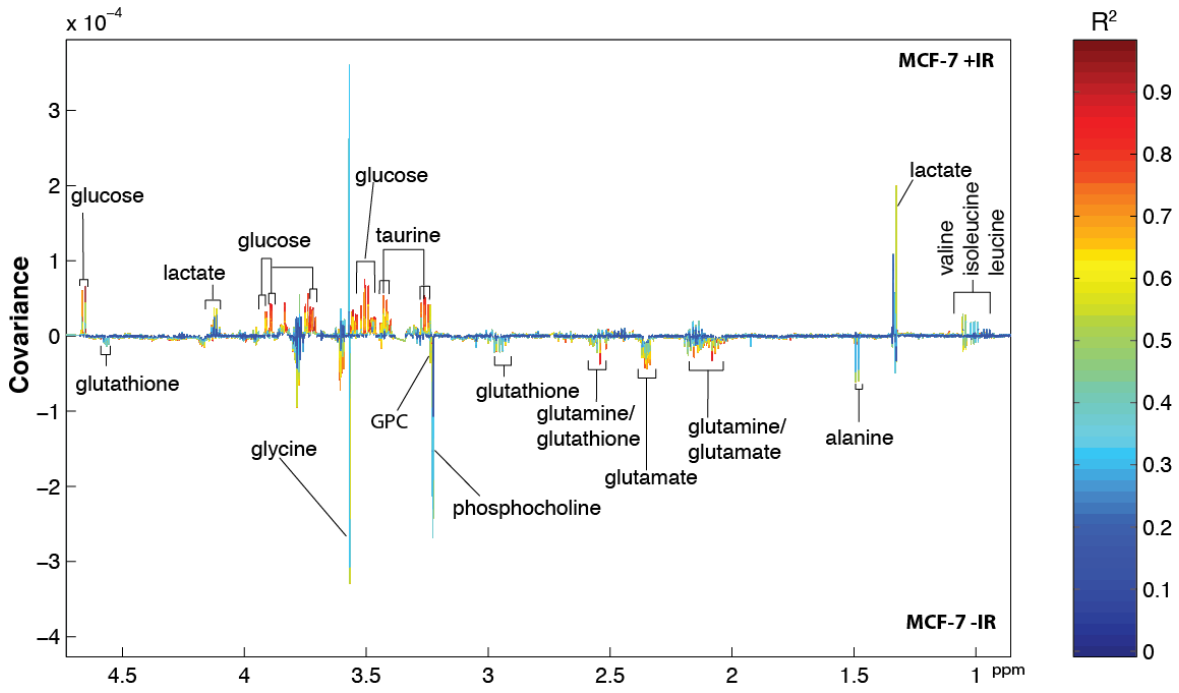

Figure 22. Correlation coefficients plot obtained from the OPLS-DA model identifying metabolic changes in the MCF-7 cells induced by 5 Gy of IR exposure. GPC, glycerophosphocholine

MCF-10A

Exposure of MCF-10A cells to IR caused a uniform metabolic response in these cells, indicated by the tight clustering in the PCA scores plot (Fig. 23A). Clear separation can be seen in the second principal component, which explains 47% of the total variation within the data. In contrast to the MCF-7 cells, irradiated MCF-10A cells had higher amounts of phosphocholine (Fig. 23B).

An OPLS-DA model with strong predictive ability ($Q^2\hat{Y}$=0.87) and valid upon permutation testing (p=0.001) was constructed to probe for the discriminating features between non-irradiated and irradiated MCF-10A cells (Fig. 24). The non-tumorigenic cells response to irradiation exposure was characterised by an increase in glutathione, this is in stark contrast to the irradiated cancer cells. Irradiation treatment also causes increases in the lactate, phosphocholine and amino acid (valine, isoleucine, leucine, alanine, threonine) content of these cells.

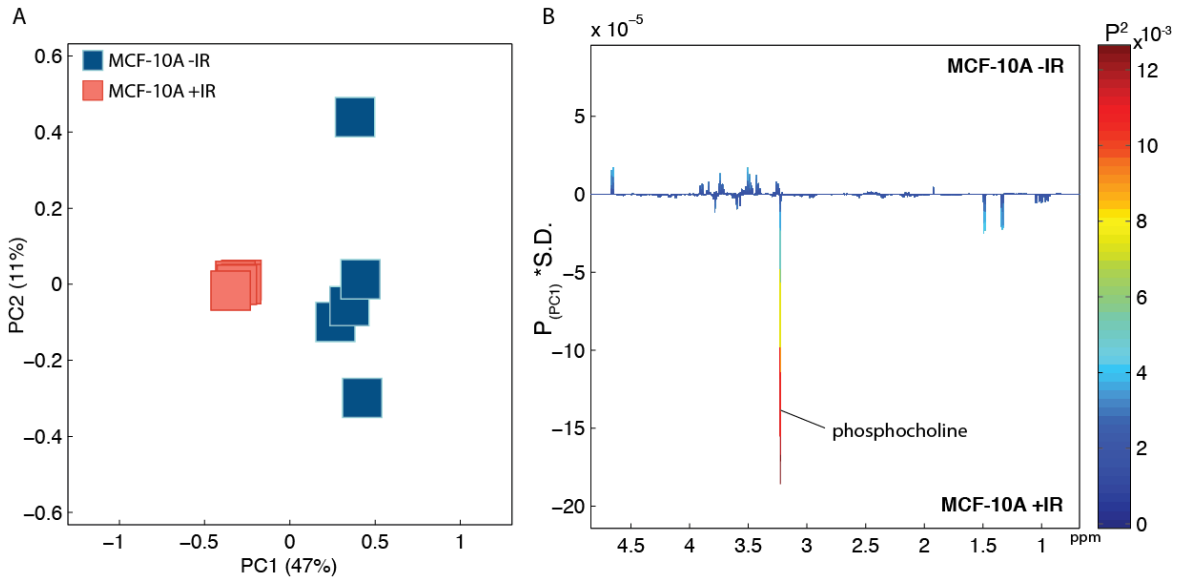

Figure 23. (A) PCA scores plot of MCF-10A untreated cells and cells exposed to 5 Gy IR. (B) PCA loadings plot for PC1.

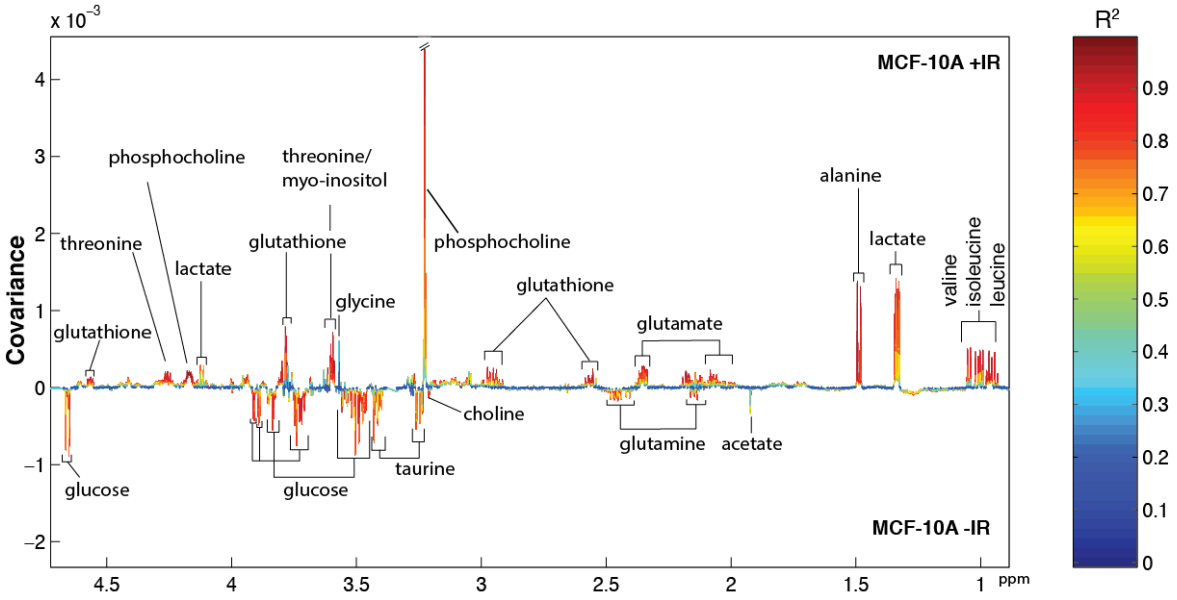

Figure 24. OPLS-DA model constructed on the metabolic profiles of cell extracts obtained from control and irradiated (5 Gy IR exposure) MCF-10A cells. GPC, glycerophosphocholine

Comparative metabolic impact of IR in MCF-7 and MCF-10A cells

Comparing the metabolic profiles of irradiated MCF-7 and MCF-10A cells returned a significant OPLS-DA model ($Q^2\hat{Y}$=0.895, *p*= 0.001) (Fig. 25). Following irradiation the metabolic differences between the cell types were consistent with the differences observed pre-treatment with higher levels of lactate, alanine, glutamine, and glycine in the MCF-7 cells. The major difference, as observed in the metabolic associations (correlation coefficients) summarised in Fig. 26, lies in the glutathione shifts between the two cell lines. At baseline, MCF-7 cells contained higher amounts of glutathione compared to MCF-10A cells however, post IR this was reversed with MCF-10A cells containing significantly higher glutathione. In addition, MCF-10A cells had significantly lower amounts of phosphocholine pre-IR compared to MCF-7 cells, but this difference was no longer significant post-IR suggesting a higher phosphocholine utilisation rate by the non-tumorigenic cell line upon IR exposure.

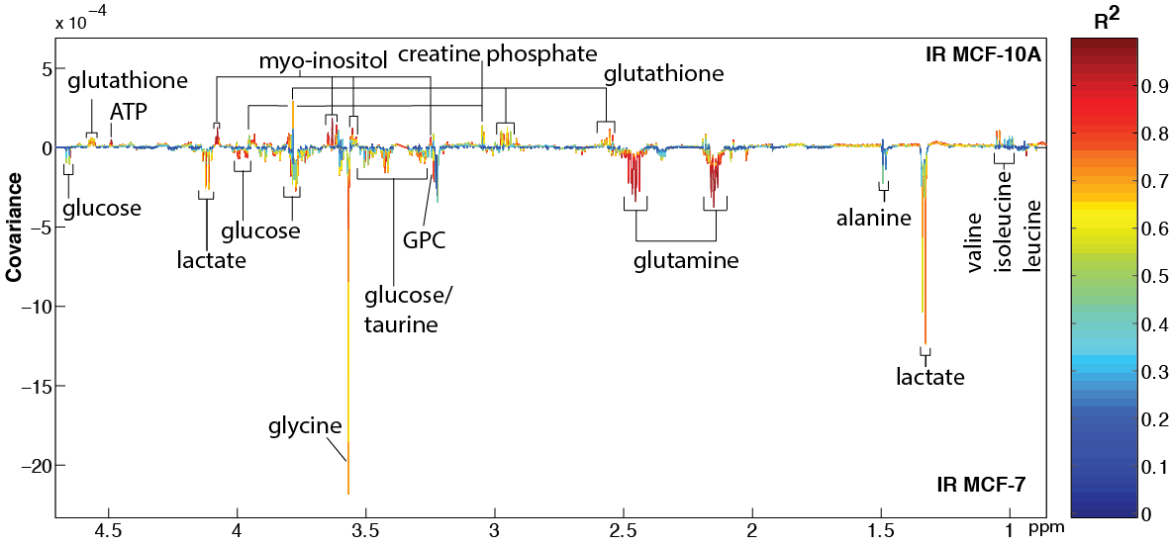

Figure 25. OPLS-DA model comparing the metabolic response of MCF-7 and MCF-10A cells exposed to 5 Gy IR. GPC, glycerophosphocholine

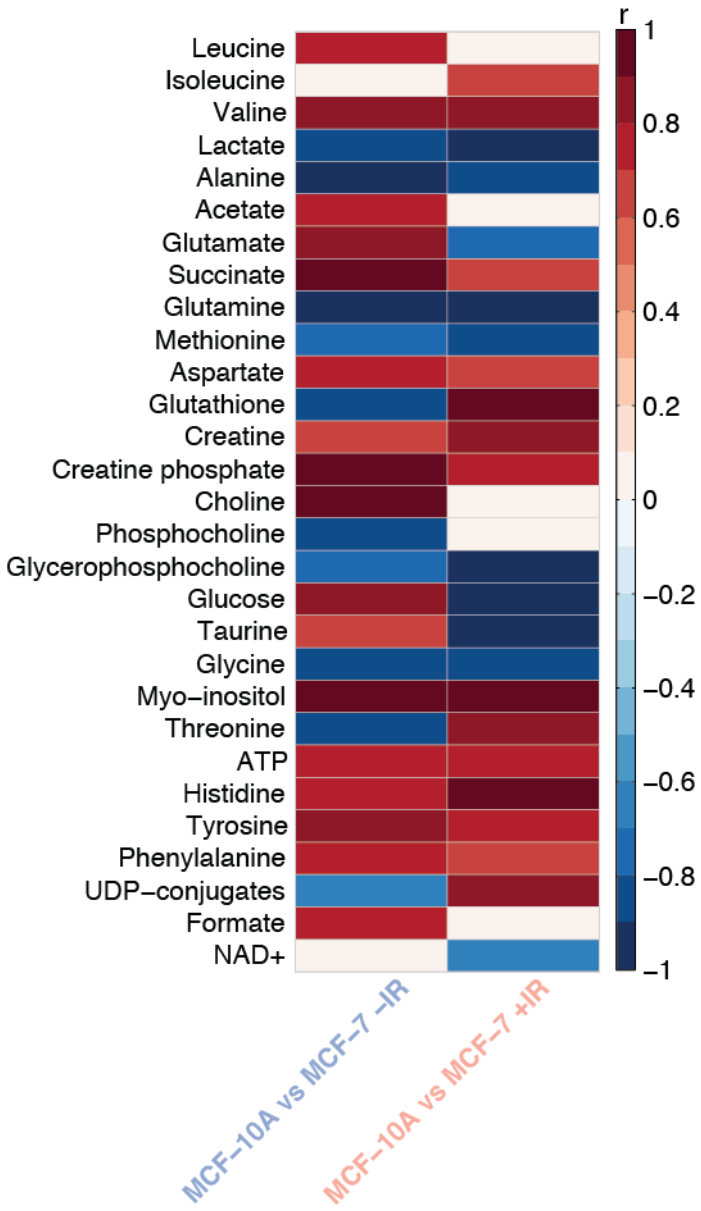

Figure 26. Summary of the significant metabolic alterations identified from the OPLS-DA models comparing metabolic profiles of MCF-7 and MCF-10A cells with (+IR) and without (-IR) radiation exposure (*n* = 5-6). Colours indicate the correlation coefficient (r) extracted from the OPLS-DA model. Red indicates metabolites that are present in higher amounts in MCF-10A cells and blue indicates metabolites that are present in lower amounts in MCF-10A cells compared to MCF-7 cells.

Metabolic perturbations induced by IR combined with PEITC or watercress extract pre-treatment

Valid OPLS-DA models with good predictive ability ($Q^2\hat{Y}$) were returned for all the pair-wise comparisons between irradiated MCF-7 and MCF-10A cells pre-treated with the different PEITC and watercress extract concentrations (Table 1). The metabolic associations between cell type and treatment and how these associations change after exposure to IR are presented in Fig. 27.

Table 2. Summary of the OPLS-DA models returned for the comparisons between irradiated control cells against cells treated with the watercress extract (12.5 or 50 µl/ml) and PEITC (10 or 20 µM) for 24 hours from both MCF-7 and MCF-10A cells.

Treatment	$R^2\hat{Y}$	$Q^2\hat{Y}$	P-value
MCF-7			
Control + IR vs WX 12.5 µl/ml	0.9650	0.6166	0.001
Control + IR vs WX 50 µl/ml	0.9749	0.6806	0.001
Control + IR vs PEITC 10µM	0.9614	0.8218	0.001
Control + IR vs PEITC 20µM	0.9410	0.6577	0.001
MCF-10A			
Control + IR vs WX 12.5 µl/ml	0.9589	0.6869	0.003
Control + IR vs WX 50 µl/ml	0.9949	0.6136	0.001
Control + IR vs PEITC 10µM	0.9259	0.7119	0.001
Control + IR vs PEITC 20µM	0.9735	0.9497	0.001

The most striking observation of the impact of the pre-treatment with PEITC or the watercress extract followed by IR, was the shift in glutathione levels in both cell lines.

We previously observed a biphasic response of MCF-7 to PEITC doses with regards to glutathione. The glutathione content of these cells was increased by low PEITC exposure (10 µM) but depleted by the high PEITC dose (20 µM). This effect remained unchanged after exposure to IR. Interestingly, in MCF-10A cells, PEITC induced elevations in the levels of

glutathione at both low and high doses, but glutathione was significantly decreased after exposure of the PEITC pre-treated cells to IR.

Crude watercress extract treatment alone, caused an increase in glutathione in MCF-7 cells and IR exposure did not affect this observation. In contrast, MCF-10A cells responded to watercress treatment with a reduction in glutathione content which was then elevated when the watercress treatment is followed by IR.

A great range of metabolic associations established during the pre-treatment of both cell lines with watercress extract and PEITC remained largely unchanged following exposure of the cells to IR including shifts in lactate, choline, taurine, glycine, UDP-conjugates as well as changes in cellular amino acid pools (Fig. 27). It should also be noted, that the metabolic signature of the MCF-10A cells pre-treated with the high PEITC dose (20 μM) combined with IR, is suggestive of a metabolic shut-down in these cells, with the majority of the metabolites being depleted.

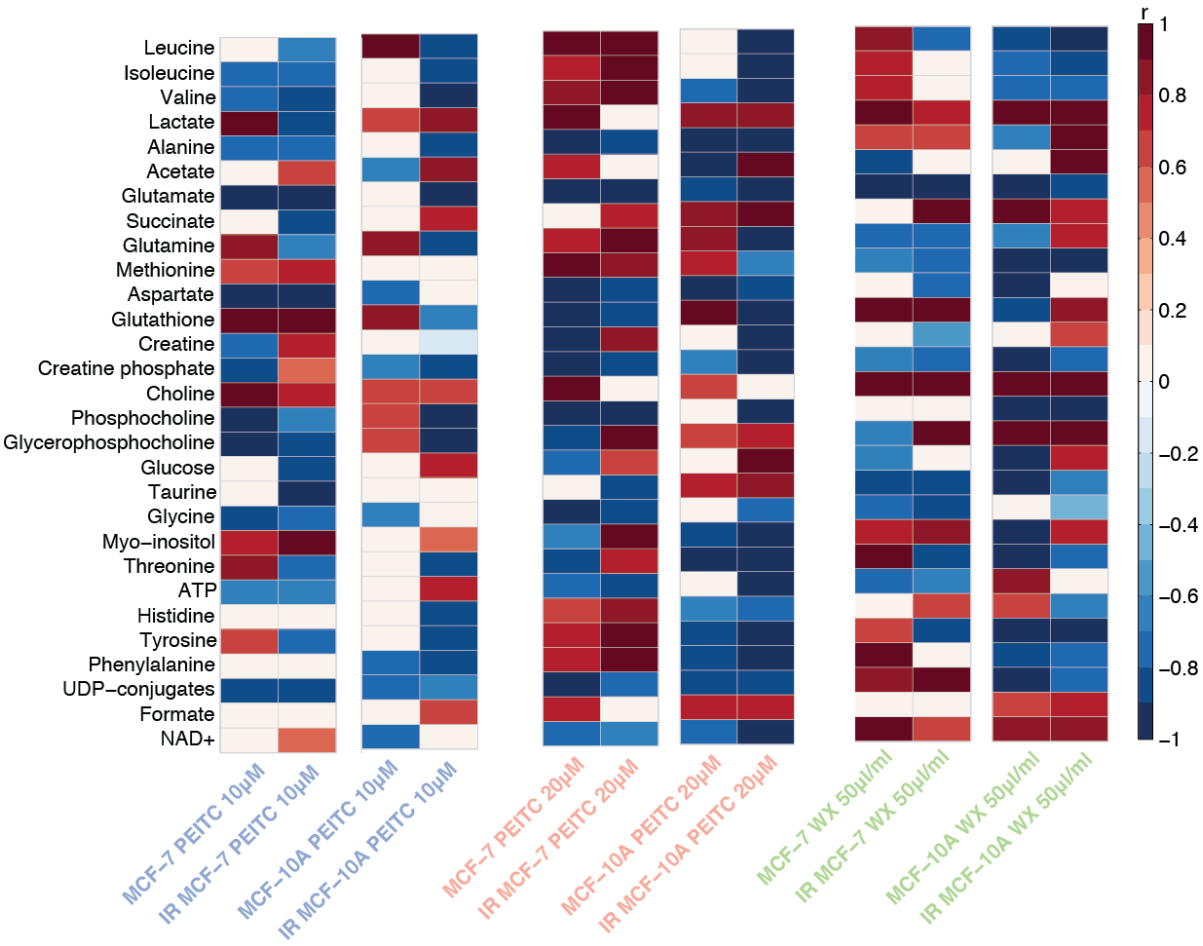

Figure 27. Summary of the metabolites associated with the OPLS-DA models given by the correlation coefficient (r) with the response variable, in this PEITC or watercress (WX) treatment and IR (*n* = 5-6). The red colour indicates metabolites that are positively correlated with the respective treatment (PEITC or WX) and blue colour indicates a negative correlation between metabolites and treatment.

Part 2 – Main findings

- Pre-treatment with PEITC sensitises cancer cells to IR induced damage as a result of glutathione depletion
- Watercress extract rescues healthy cells from IR collateral damage by modulating glutathione levels and inducing anti-oxidant mechanisms.

Results – Part 3

Effects of domestic processing methods on the phytochemical content of watercress (Nasturtium officinale)

The profiles obtained from microwaved and steamed watercress closely resembled that of fresh watercress with these cooking methodologies positively correlating with the phenolics, carotenoids and glucosinolate concentrations. In stark contrast, boiled watercress has a phytochemical profile very different from that of fresh watercress characterised by elevated carotenoid amounts and significant losses in glucosinolates and flavonols, which essentially result in compromised antioxidant activity. Chopped watercress and watercress smoothie samples have similar phytochemical profiles and separate from the fresh samples on the first principal component characterised by losses of all the phytochemicals quantified in our study. Cooking time appears to be negatively correlated with microwaving, boiling and steaming but exposure of chopped samples and watercress smoothie to ambient temperature for extended time periods does not appear to have a particular impact on the measureable phytochemicals in these samples, expect in the total phenolic content of stored chopped watercress. Antioxidant activity as measured by the FRAP assay, exhibits a significant positive correlation with microwaving driven by higher concentrations of glucosinolates and flavonols suggesting that it should be the preferred method of watercress preparation when it is not consumed raw. PCA reveals distinct phytochemical profiles for watercress cooked using different regimes (Fig. 28).

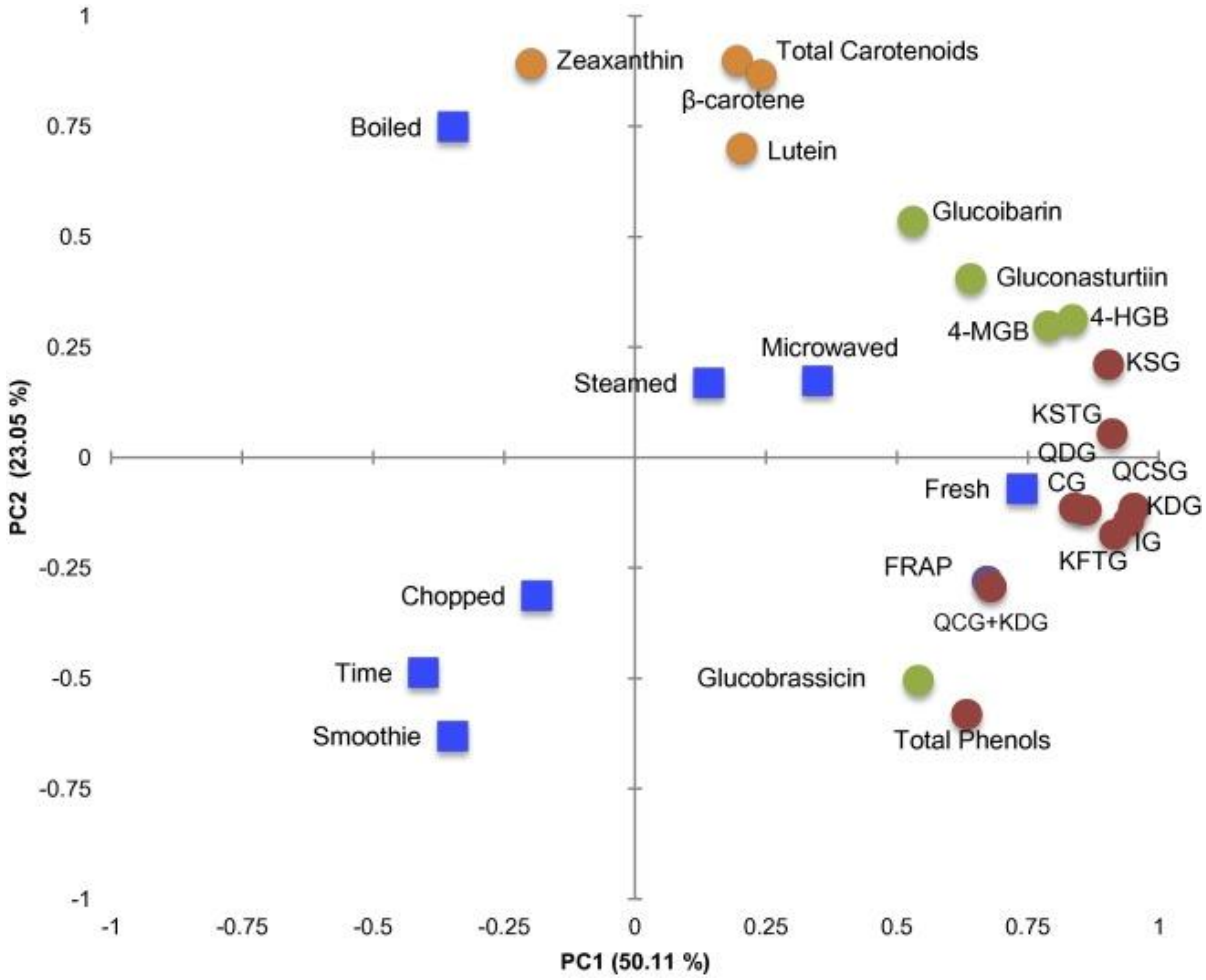

Figure 28 PCA scores of all cooked samples (□) and loadings plot for all quantified phytochemicals (○). Abbreviations: 4-MGB, 4-methoxyglucobrassicin; 4-HGB, 4-hydroxyglucobrassicin; KSG, K 3-(sinp-Glc)-4′Glc; KSTG, K 3-(sinp-triGlc)-7-Glc; QDGCG, QCSG, Q 3-(caf-Glc)-3′-(sinp-Glc)-4′-Glc; KDG, K 3-diGlc-7-Glc; IG, I 3-Glc; KFTG, K 3-(fer-triGlc)-7 Glc; QCG + KDG Q 3,4′diGlc-3′-(p.coum-Glc) + K 3,4′-diGlc

Part 3 – Main findings

- Cooking has a significant impact on the density and diversity of watercress phytochemicals
- Steaming and microwaving are the recommended methods for watercress preparation because they maintain the majority of phytochemicals in comparison to fresh watercress
- Boiling of watercress should be avoided to ensure maximum ingestions of nutrients

Discussion

Summary of main findings

- Crude watercress extract and PEITC induce notable metabolic perturbations in MCF-7 and MCF-10A cells.
- Watercress and PEITC compromise cell proliferation in MCF-7 cells, and a 30 μM dose of PEITC is cytotoxic to MCF-10A cells.
- PEITC and watercress induce G1 and S phase cell cycle arrest in MCF-7 cells respectively.
- Watercress extract is not a genotoxic agent but PEITC damages MCF-7 cells as well as MCF-10A cells to a lesser extent.
- Mitochondrial membrane potential is significantly compromised by watercress and PEITC in MCF-7 cells and in MCF-10A cells treated with the higher doses of PEITC.
- Pre-treatment with PEITC sensitises cancer cells to IR induced damage as a result of glutathione depletion
- Watercress extract rescues healthy cells from IR collateral damage by modulating glutathione levels and inducing anti-oxidant mechanisms

Crude watercress extract and PEITC induced a range of phenotypic changes in cell behaviour both in MCF-7 and MCF-10A cells. The concentrations of PEITC used in this study are achievable *in vivo* by consuming 100 g of watercress (Cheung and Kong, 2010) and are known to have *in vitro* anti-cancer activity (Cavell *et al.,* 2012). ^{1}H-NMR spectroscopy based metabonomics was successfully applied to tumorigenic MCF-7 and non-tumorigenic MCF-10A breast cells to examine the fundamental differences in their metabolic phenotype. The biochemical impact of crude watercress extract and PEITC was examined on these two cell lines. To our knowledge this is the first study looking at the comparative metabolic responses of these cell lines to bioactive compounds of nutritional importance. The responses of the two cell lines to the treatments are following three main metabolic trajectories involving glutathione shifts, glucose and phosphocholine metabolism corresponding to functions of oxidative stress, energy maintenance and cell proliferation respectively.

Glutathione

The MCF-7 breast cancer cells exhibited non-linear but dose-dependent changes in glutathione concentrations in response to watercress and PEITC treatments. PEITC appears to induce a biphasic response in the glutathione abundance of MCF-7 cells, with increased concentrations at low doses and depletion at the two higher doses. The ability of isothiocyanates to act as both pro-oxidants and indirect antioxidants may explain the dose-dependent fluctuations in cellular glutathione content. Prolonged exposure to low isothiocyanate concentrations can induce phase II enzymes, which regulate antioxidant gene expression (Dinkova-Kostova and Kostov, 2012) potentially explaining the increase in glutathione observed in the MCF-7 cells treated with the lower doses of PEITC. PEITC effectively depletes cells of glutathione by continued intracellular conjugation and efflux (Fig. 1) hence disabling the glutathione antioxidant system (Zhang, 2001, Zhang, 2000). Glutathione depletion accompanied by compromised mitochondrial function ultimately results in excessive oxidative stress, as demonstrated by the increased levels of DNA damage with higher PEITC exposure and this may help explain the observed cell cycle arrest and cell cytotoxicity in the PEITC treated MCF-7 cells. Interestingly, PEITC did not deplete MCF-10A cells of glutathione, despite comparable basal glutathione levels between the two cell lines, and these cells were also less sensitive to PEITC induced DNA damage. PEITC has previously been shown to selectively kill cancer cells with lower antioxidant status over non-tumorigenic cell lines (Trachootham *et al*., 2006, Powolny and Singh, 2010, Hong *et al*., 2015)

Glutathione increased in MCF-7 cells with increasing concentrations of the watercress extract. This is likely to be a result of the complex mixture of compounds in the watercress extract such as phenolics and flavonoids with proven antioxidant properties. Flavonoids increase the expression of γ-glutamylcysteine synthetase, which is directly proportional to elevated glutathione levels (Moskaug *et al*., 2005). Watercress is also a rich source of folate (USDA, 2013) which can be used in one-carbon metabolism pathway, adding to the cellular glutathione pool.

Different responses were observed in glutathione abundance following IR exposure in MCF-7 versus MCF-10A cells. Treatment of MCF-7 cells with IR resulted in intracellular glutathione depletion in agreement with other studies where important decreases in glutathione were observed in cancer cells exposed to IR (Rainaldi *et al*., 2008, Bell and Wagstaff, 2014, Rosi *et al*., 2007). In contrast, MCF-10A cells responded to IR induced stress by increasing their glutathione content. IR generates reactive oxygen species ROS, which are quenched in part through the glutathione response reducing the potential of ROS to exert oxidative DNA damage. Elevations in intracellular glutathione in MCF-10A cells can be considered part of a protective response by up-regulating the metabolic anti-oxidant capacity of these cells. This

may explain their ability to better recover from IR induced damage compared to MCF-7 cells, and which may explain the lower levels of DNA damage observed in the healthy cells in this study.

MCF-10A cells responded to low dose PEITC treatment (10 µM) by elevating their glutathione content. When these cells were exposed to IR and PEITC (10 µM), glutathione was depleted contrary to situation in the cancer cells. Deleted glutathione pools suggest increased utilisation of glutathione for IR-derived ROS scavenging purposes, explaining the decreased DNA damage levels in these cells.

Pre-treatment of MCF-10A cells with the watercress extract also appeared to be protective when the cells were exposed to IR, evidenced by the reduced levels of DNA damage. Watercress extract has been shown to possess anti-genotoxic properties in several in vitro models where cells have been challenged with known genotoxic agents (Kassie *et al*., 2003, Boyd *et al*., 2006). The combined treatment of MCF-10A cells with the watercress extract and IR appeared to increase the glutathione content of these cells, suggestive of enhanced anti-oxidant activity and hence a protective effect.

The metabolic signatures of MCF-7 cells indicate that glutathione depletion is a major target for PEITC, which can lead to the build up of intracellular ROS resulting in cell damage. Elevated ROS is a characteristic outcome of IR exposure and, combined with the glutathione-depleting property of PEITC, could be exploited for cancer cell killing. Indeed, our results suggest that PEITC treatment can sensitise cells to IR induced damage as observed from G1 cell cycle arrest, elevated DNA damage levels and reduced cell viability.

Phosphocholine metabolism

Cellular membranes are a primary target of IR due to the impact ROS can have on lipid bilayers of which phosphocholine is a main constituent. Scavenging of ROS by the higher levels of glutathione observed in MCF-10A cells can explain the apparent increase in their phosphocholine levels. This may reflect the efforts to maintain cell membrane integrity, which can be violated by ROS produced as a result of IR exposure. Conversely, the MCF-7 response to IR was characterised by lower levels of phosphocholine. Phosphocholine can potentially serve as a breast cancer biomarker since higher levels of this molecule have been reported in the clinical setting in breast cancer lesions compared to benign breast cancer lesions (Katz-Brull *et al*., 2002, Bolan *et al*., 2003, Meisamy *et al*., 2005) as well as *in vitro* in comparisons of cancerous cell with normal mammary epithelial cells (Eliyahu *et al*., 2007). Decreases in phosphocholine have been observed in tissues after chemotherapy and radiation treatment and have been correlated with positive therapy outcomes (Sijens *et al*., 1995, Lindskog *et al*., 2005, Podo, 1999, Rainaldi *et al*., 2008).

PEITC treatment reduced phosphocholine abundance suggesting an impact on cell membrane integrity that may contribute to radiation-induced cancer cell killing. However, this effect is not limited to the tumorigenic landscape. The high dose of PEITC combined with IR was genotoxic to healthy cells, characterised by DNA damage and apparent reduced metabolic activity, providing further evidence to the hormetic behaviour of dietary isothiocyanates (Bao *et al*., 2014).

Energy status, glycolysis and mitochondrial function

The ‘’Warburg effect’’ is the most well established metabolic phenotype observed in cancer cells. It postulates that tumour cells generate ATP through enhanced glycolysis rather than oxidative phosphorylation, characterised by higher lactate as seen here in MCF-7 cells, even when oxygen is not a limiting factor and although they have possess the functional properties to maintain oxidative phosphorylation. As a result the majority of the glucose is converted to lactate via glycolysis, providing a rapid source of ATP. However, this is a far less efficient process in terms of ATP molecules produced per mol of glucose input.

Results from the mitochondrial membrane potential assay indicate that the watercress extract and PEITC significantly compromise mitochondrial function. Oxidative phosphorylation can therefore no longer occur in the mitochondria resulting in cellular energy depletion. Up regulated glycolysis, evident by increased lactate levels, is an essential adaptation to cope with the limited capacity for ATP generation through oxidative phosphorylation. Pyruvate dehydrogenase (PDH) kinase is inhibited by increasing concentrations of ROS, which may increase as a result of the observed glutathione depletion (Hurd *et al*., 2012). PDH kinase catalyses the conversion of pyruvate to acetyl-coA dictating the rate at which the TCA cycle occurs and its inhibition may therefore favour lactate production (Hurd *et al*., 2012).

Combined treatment of MCF-7 cells with the high PEITC dose (20 µM) and IR was also characterised by sparing of glucose and reduced lactate abundance, suggesting that the rates of glycolysis were diminished. Glycolysis is the main source of energy and biosynthetic molecules in cancer cells. Attenuated activity of this pathway further adds to the cancer killing process.

Conclusions

^{1}H-NMR metabonomics has been successfully applied in profiling and distinguishing between tumorigenic and non-transformed cells as well as mapping the responses of MCF-7 and MCF-10A breast cells to PEITC and crude watercress extract with and without IR. Our results suggest that the most prominent metabolic targets of the two treatments include glutathione metabolism, energy metabolism as well as phospholipid and amino acid metabolism. Metabolic biomarkers identified in this study provide further evidence on the biphasic impact that PEITC has on the oxidative status on breast cancer cells and that the observed effects are distinct between malignant and normal cells. Watercress and PEITC can induce significant changes in the cancer cell metabonome accompanied by genotoxic effects such as cell cycle arrest, mitochondrial damage and oxidative stress.

Combined treatment of breast cells with IR as well as PEITC or the watercress extract suggest a potential synergistic effect of PEITC and IR towards MCF-7 cell killing and radio-sensitisation and that PEITC – free watercress extract can rescue healthy cells from collateral damage. It is postulated that glutathione has a principal role in the response of cells to IR challenge and that the inclusion of dietary watercress during radiotherapy may enhance the outcome.

Our study also clearly demonstrates that health-promoting compounds in watercress are significantly influenced by domestic processing methods. Cooking by microwaving and steaming preserves the levels of most phytochemicals in watercress. Domestic processing can have a detrimental effect on the bioactives, which may be responsible for the health promoting properties of watercress. Satisfactory retention of beneficial phytochemicals in watercress may be achieved by avoiding boiling which results in a compromised phytochemical profile.

Study limitations and future perspectives

The work described in report, has addressed a number of research questions, while highlighting some opportunities for future research. Further work would advance our understanding regarding the molecular mechanisms of action of watercress and PEITC in cancer and provide further data on the relevance of watercress consumption during breast cancer therapy *in vivo*.

Breast cancer is a highly heterogeneous disease, with distinct molecular sub-types leading to differential responses to target therapies. The experiments in this project were carried out using MCF-7 breast cancer cells and MCF-10A healthy cells. MCF-10A cells are the most commonly used healthy breast cells and represent the best model for the study of normal

human mammary epithelial function available to date. On the other hand, MCF-7 cells represent only one molecular sub-type of breast cancer. Consequently, further work should be carried out to examine whether the findings from the experiments carried out in this thesis are consistent with other *in vitro* models of breast cancer, which represent different degrees of sensitivity, endocrine responsiveness, metastatic potential and immunoprofile.

In the initial parts of the *in vitro* work significant shifts in the levels of lactate were observed upon treatment with watercress and PEITC in both cells lines suggestive of disruptions in oxidative and glycolytic metabolism. Increased lactate is postulated to arise from a compromised ability for oxidative phosphorylation due to mitochondrial membrane damage and a switching of cells to glycolysis as a last resort for energy acquisition. As discussed previously glycolysis is a key pathway in cancer cell metabolism, therefore further work is recommended to elucidate the mechanism behind our observation. Real-time rates of oxidative phosphorylation and glycolysis can be studied using Seahorse Cell Analysis™, which provides functional cellular metabolic data. Furthermore, experiments using radiolabeled glucose isotopes to study glucose uptake and metabolism combined with glucose and lactate transporters expression data could provide a more mechanistic overview on the impact of watercress and PEITC on glucose cellular energetics.

In the IR *in vitro* experiments a protective effect of watercress against radiation induced damage in healthy breast cells was observed parallel to a radio-sensitising impact of PEITC in breast cancer cells. Cell cycle and Comet assay data supported these observations, however additional experiments are required to further explore these effects. Transcriptomics for the interrogation of DNA damage, apoptosis, as well as repair pathways would further our understanding of the chemo-protective effect of watercress and the genotoxic effect of PEITC. Information obtained from such an exploratory approach could be integrated with metabonomic data and provide a better picture of the interactions between genetic, metabolic and physiological shifts in an irradiation-perturbed system.

Despite obtaining encouraging results from the *in vitro* work performed; the results could not be validated *in vivo* therefore the relevance of our observations remains to be examined. This was a consequence of an inadequate study design, characterised by low participant numbers, as well as an incorrect randomisation strategy. A clinical trial investigating the impact of watercress consumption during radiotherapy should be performed. It is recommended that the study should be performed at a hospital with a high intake of breast cancer patients to allow for the recruitment of enough volunteers to adequately power the study. The study design should consist of four treatment groups: a) healthy individuals on their habitual diet, b) healthy individuals consuming watercress, c) breast cancer patients undergoing radiotherapy without consuming watercress and d) breast cancer patients consuming

watercress throughout their radiotherapy treatment. Collection of plasma and urine samples from volunteers in these groups would help draw meaningful conclusions on the metabolic fingerprint of breast cancer, radiotherapy and a nutritional intervention through watercress ingestion. Pre-screening of the participants prior to their participation in the clinical trial is of paramount importance to avoid the introduction of bias from differences in anthropometric and physiological factors. In addition, a proper randomisation method should be employed to ensure the acquisition of valid and interpretable results.

Closing remark

This thesis has provided evidence for the potential of watercress and PEITC to induce significant metabolic perturbations in breast cancer, a previously unexplored area. Novel preliminary evidence have been obtained, for the potential prophylactic impact of watercress during radiotherapy, through protecting healthy tissue from damage as well as enhancing the therapeutic outcomes of the treatment. The systemic impact of watercress against breast cancer should be further explored, for the generation of robust evidence in support of the current, promising findings.

Knowledge and Technology Transfer

Knowledge transfer activities involve presenting the work carried out in conferences and academic publications. Scientific posters of this work have been presented in the Glucosinolates conference in Wageningen October 2014, and the Metabolomics society meeting in London in September 2014. The work has also been presented in seminar series at the University of Reading (2015 and 2016) as well as the Doctoral conference at the University of Reading (2015). A manuscript entitled ‘’Effects of domestic processing methods on the phytochemical content of watercress (*Nasturtium officinale)”* has been published in the Journal of Food Chemistry (reference and link in appendix). Two additional manuscripts are in preparation, presenting the *in vitro* work carried out and will be submitted in the near future.

Glossary

Metabolites: small biological compounds involved in biochemical processes and pathways. Examples include cholesterol, glucose and amino acids

Metabolome: A collection of all metabolites observed in a biological system under a given set of conditions.

Metabolomics: the analysis, quantification and interpretation of metabolite levels in biological samples with the aim of characterising the metabolome.

Metabonomics: The study of changes in metabolite levels in response to drugs, diseases or toxicity, usually used when determining such changes using NMR.

Metabolic profiling: Analysis of a group of metabolites that are a part of a particular group or class (e.g. sugars, lipids) or linked to a specific pathway.

NMR spectroscopy: Some atomic nuclei possess a non-zero magnetic moment. This property is quantised and leads to discrete energy states in a magnetic field. Nuclei such as 1H, 13C, 15N, 19F and 31P can undergo transitions between these states when radiofrequency pulses of appropriate energy are applied. The exact frequency of a transition depends on the type of nucleus and on its electronic environment in a molecule. For example, 1H nuclei in a molecule give NMR peaks at frequencies (chemical shifts) characteristic of their chemical environment. In metabonomics, it is the patterns that occur when many different biochemical entities are detected simultaneously in a mixture using 1H NMR that are interpreted

Principal component analysis (PCA): PCA is an unsupervised data visualisation method that is useful for observing groupings within multivariate data. NMR data are presented in n dimensional space, where n is the number of variables (metabolites in this case), and it reduced into a few principal components, which are descriptive dimensions that describe the maximum variation in the data. The principal components can be displayed in a graphical fashion as 'scores' plot. This plot is useful for observing any groupings in the data set. Coefficients by which the original variables must be multiplied to obtain the PC are called 'loadings'. The numerical value on a PC shows how much the variable has in common with that component. Thus loadings plots can be used to detect the spectral areas (metabolite's peaks) responsible for the groupings/ separation in the data.

Projections to latent structures (PLS): Supervised methods incorporate additional information relating to the data set, such as class membership or qualitative responses, and are used to make predictions based on the data. PLS and PLS–discriminant analysis (PLS-DA) are two commonly applied supervised methods. With PLS-DA, latent variables (scores and loadings pairs) are calculated to optimize the covariance between the (spectroscopic) data and class assignment (pre- and post-intervention).

References

BAO, Y., WANG, W., ZHOU, Z. & SUN, C. 2014. Benefits and risks of the hormetic effects of dietary isothiocyanates on cancer prevention. *PLoS One,* 9**,** e114764.

BELL & WAGSTAFF, C. 2014. Glucosinolates, Myrosinase Hydrolysis Products, and Flavonols Found in Rocket (Eruca sativa and Diplotaxis tenuifolia). *Journal of Agricultural and Food Chemistry,* 62**,** 4481-4492.

BOGGS, D. A., PALMER, J. R., WISE, L. A., SPIEGELMAN, D., STAMPFER, M. J., ADAMS-CAMPBELL, L. L. & ROSENBERG, L. 2010. Fruit and vegetable intake in relation to

risk of breast cancer in the Black Women's Health Study. *Am J Epidemiol,* 172**,** 1268-79.
BOLAN, P. J., MEISAMY, S., BAKER, E. H., LIN, J., EMORY, T., NELSON, M., EVERSON, L. I., YEE, D. & GARWOOD, M. 2003. In vivo quantification of choline compounds in the breast with 1H MR spectroscopy. *Magn Reson Med,* 50**,** 1134-43.
BOYD, L. A., MCCANN, M. J., HASHIM, Y., BENNETT, R. N., GILL, C. I. & ROWLAND, I. R. 2006. Assessment of the anti-genotoxic, anti-proliferative, and anti-metastatic potential of crude watercress extract in human colon cancer cells. *Nutr Cancer,* 55**,** 232-41.
CAIRNS, R. A., HARRIS, I. S. & MAK, T. W. 2011. Regulation of cancer cell metabolism. *Nat Rev Cancer,* 11**,** 85-95.
CAVELL, B. E., SYED ALWI, S. S., DONLEVY, A. & PACKHAM, G. 2011. Anti-angiogenic effects of dietary isothiocyanates: mechanisms of action and implications for human health. *Biochem Pharmacol,* 81**,** 327-36.
CAVELL, B. E., SYED ALWI, S. S., DONLEVY, A. M., PROUD, C. G. & PACKHAM, G. 2012. Natural product-derived antitumor compound phenethyl isothiocyanate inhibits mTORC1 activity via TSC2. *J Nat Prod,* 75**,** 1051-7.
CHEUNG, K. L., KHOR, T. O., YU, S. & KONG, A. N. 2008. PEITC induces G1 cell cycle arrest on HT-29 cells through the activation of p38 MAPK signaling pathway. *AAPS J,* 10**,** 277-81.
CHEUNG, K. L. & KONG, A. N. 2010. Molecular targets of dietary phenethyl isothiocyanate and sulforaphane for cancer chemoprevention. *AAPS J,* 12**,** 87-97.
DINKOVA-KOSTOVA, A. T. & KOSTOV, R. V. 2012. Glucosinolates and isothiocyanates in health and disease. *Trends Mol Med,* 18**,** 337-47.
EISA, N. H., ELSHERBINY, N. M., SHEBL, A. M., EISSA, L. A. & EL-SHISHTAWY, M. M. 2015. Phenethyl isothiocyanate potentiates anti-tumour effect of doxorubicin through Akt-dependent pathway. *Cell Biochem Funct,* 33**,** 541-51.
ELIYAHU, G., KREIZMAN, T. & DEGANI, H. 2007. Phosphocholine as a biomarker of breast cancer: molecular and biochemical studies. *Int J Cancer,* 120**,** 1721-30.
FOGARTY, M. C., HUGHES, C. M., BURKE, G., BROWN, J. C. & DAVISON, G. W. 2013. Acute and chronic watercress supplementation attenuates exercise-induced peripheral mononuclear cell DNA damage and lipid peroxidation. *Br J Nutr,* 109**,** 293-301.
GIALLOUROU, N., ORUNA-CONCHA, M. J. & HARBOURNE, N. 2016. Effects of domestic processing methods on the phytochemical content of watercress (Nasturtium officinale). *Food Chem,* 212**,** 411-9.
GILL, C. I. R., HALDAR, S., BOYD, L. A., BENNETT, R., WHITEFORD, J., BUTLER, M., PEARSON, J. R., BRADBURY, I. & ROWLAND, I. R. 2007. Watercress supplementation in diet reduces lymphocyte DNA damage and alters blood antioxidant status in healthy adults. *American Journal of Clinical Nutrition,* 85**,** 504-510.
HONG, Y. H., UDDIN, M. H., JO, U., KIM, B., SONG, J., SUH, D. H., KIM, H. S. & SONG, Y. S. 2015. ROS Accumulation by PEITC Selectively Kills Ovarian Cancer Cells via UPR-Mediated Apoptosis. *Front Oncol,* 5**,** 167.
HU, Y., ROSEN, D. G., ZHOU, Y., FENG, L., YANG, G., LIU, J. & HUANG, P. 2005. Mitochondrial manganese-superoxide dismutase expression in ovarian cancer: role in cell proliferation and response to oxidative stress. *J Biol Chem,* 280**,** 39485-92.
HURD, T. R., COLLINS, Y., ABAKUMOVA, I., CHOUCHANI, E. T., BARANOWSKI, B., FEARNLEY, I. M., PRIME, T. A., MURPHY, M. P. & JAMES, A. M. 2012. Inactivation of pyruvate dehydrogenase kinase 2 by mitochondrial reactive oxygen species. *J Biol Chem,* 287**,** 35153-60.
JEONG, W. S., KIM, I. W., HU, R. & KONG, A. N. 2004. Modulatory properties of various natural chemopreventive agents on the activation of NF-kappaB signaling pathway. *Pharm Res,* 21**,** 661-70.

KARIN, M. 2006. Nuclear factor-kappaB in cancer development and progression. *Nature,* 441**,** 431-6.
KASSIE, F., LAKY, B., GMINSKI, R., MERSCH-SUNDERMANN, V., SCHARF, G., LHOSTE, E. & KANSMULLER, S. 2003. Effects of garden and water cress juices and their constituents, benzyl and phenethyl isothiocyanates, towards benzo(a)pyrene-induced DNA damage: a model study with the single cell gel electrophoresis/Hep G2 assay. *Chem Biol Interact,* 142**,** 285-96.
KATZ-BRULL, R., LAVIN, P. T. & LENKINSKI, R. E. 2002. Clinical utility of proton magnetic resonance spectroscopy in characterizing breast lesions. *J Natl Cancer Inst,* 94**,** 1197-203.
LINDSKOG, M., SPENGER, C., KLASON, T., JARVET, J., GRASLUND, A., JOHNSEN, J. I., PONTHAN, F., DOUGLAS, L., NORDELL, B. & KOGNER, P. 2005. Proton magnetic resonance spectroscopy in neuroblastoma: current status, prospects and limitations. *Cancer Lett,* 228**,** 247-55.
LIU, X. & LV, K. 2013. Cruciferous vegetables intake is inversely associated with risk of breast cancer: a meta-analysis. *Breast,* 22**,** 309-13.
MEISAMY, S., BOLAN, P. J., BAKER, E. H., POLLEMA, M. G., LE, C. T., KELCZ, F., LECHNER, M. C., LUIKENS, B. A., CARLSON, R. A., BRANDT, K. R., AMRAMI, K. K., NELSON, M. T., EVERSON, L. I., EMORY, T. H., TUTTLE, T. M., YEE, D. & GARWOOD, M. 2005. Adding in vivo quantitative 1H MR spectroscopy to improve diagnostic accuracy of breast MR imaging: preliminary results of observer performance study at 4.0 T. *Radiology,* 236**,** 465-75.
MOSKAUG, J. O., CARLSEN, H., MYHRSTAD, M. C. & BLOMHOFF, R. 2005. Polyphenols and glutathione synthesis regulation. *Am J Clin Nutr,* 81**,** 277S-283S.
PODO, F. 1999. Tumour phospholipid metabolism. *NMR Biomed,* 12**,** 413-39.
POWOLNY, A. A. & SINGH, S. V. 2010. Differential response of normal (PrEC) and cancerous human prostate cells (PC-3) to phenethyl isothiocyanate-mediated changes in expression of antioxidant defense genes. *Pharm Res,* 27**,** 2766-75.
RAINALDI, G., ROMANO, R., INDOVINA, P., FERRANTE, A., MOTTA, A., INDOVINA, P. L. & SANTINI, M. T. 2008. Metabolomics using 1H-NMR of apoptosis and Necrosis in HL60 leukemia cells: differences between the two types of cell death and independence from the stimulus of apoptosis used. *Radiat Res,* 169**,** 170-80.
ROSE, P., FAULKNER, K., WILLIAMSON, G. & MITHEN, R. 2000. 7-Methylsulfinylheptyl and 8-methylsulfinyloctyl isothiocyanates from watercress are potent inducers of phase II enzymes. *Carcinogenesis,* 21**,** 1983-8.
ROSE, P., HUANG, Q., ONG, C. N. & WHITEMAN, M. 2005a. Broccoli and watercress suppress matrix metalloproteinase-9 activity and invasiveness of human MDA-MB-231 breast cancer cells. *Toxicol Appl Pharmacol,* 209**,** 105-13.
ROSE, P., WON, Y. K., ONG, C. N. & WHITEMAN, M. 2005b. Beta-phenylethyl and 8-methylsulphinyloctyl isothiocyanates, constituents of watercress, suppress LPS induced production of nitric oxide and prostaglandin E2 in RAW 264.7 macrophages. *Nitric Oxide,* 12**,** 237-43.
ROSI, A., GRANDE, S., LUCIANI, A. M., PALMA, A., GIOVANNINI, C., GUIDONI, L., SAPORA, O. & VITI, V. 2007. Role of glutathione in apoptosis induced by radiation as determined by 1H MR spectra of cultured tumor cells. *Radiat Res,* 167**,** 268-82.
SIJENS, P. E., VECHT, C. J., LEVENDAG, P. C., VAN DIJK, P. & OUDKERK, M. 1995. Hydrogen magnetic resonance spectroscopy follow-up after radiation therapy of human brain cancer. Unexpected inverse correlation between the changes in tumor choline level and post-gadolinium magnetic resonance imaging contrast. *Invest Radiol,* 30**,** 738-44.
SYED ALWI, S. S., CAVELL, B. E., DONLEVY, A. & PACKHAM, G. 2012. Differential induction of apoptosis in human breast cancer cell lines by phenethyl isothiocyanate, a glutathione depleting agent. *Cell Stress Chaperones,* 17**,** 529-38.
TRACHOOTHAM, D., ZHOU, Y., ZHANG, H., DEMIZU, Y., CHEN, Z., PELICANO, H., CHIAO, P. J., ACHANTA, G., ARLINGHAUS, R. B., LIU, J. S. & HUANG, P. 2006.

Selective killing of oncogenically transformed cells through a ROS-mediated mechanism by beta-phenylethyl isothiocyanate. *Cancer Cell,* 10**,** 241-252.
USDA 2013. USDA Nutrient Data Laboratory. *Choice: Current Reviews for Academic Libraries,* 42**,** 153-153.
VAUGHN, A. E. & DESHMUKH, M. 2008. Glucose metabolism inhibits apoptosis in neurons and cancer cells by redox inactivation of cytochrome c. *Nat Cell Biol,* 10**,** 1477-83.
VERHOEVEN, D. T. H., GOLDBOHM, R. A., VANPOPPEL, G., VERHAGEN, H. & VANDENBRANDT, P. A. 1996. Epidemiological studies on brassica vegetables and cancer risk. *Cancer Epidemiology Biomarkers & Prevention,* 5**,** 733-748.
WANG, X., GOVIND, S., SAJANKILA, S. P., MI, L., ROY, R. & CHUNG, F. L. 2011. Phenethyl isothiocyanate sensitizes human cervical cancer cells to apoptosis induced by cisplatin. *Mol Nutr Food Res,* 55**,** 1572-81.
WANG, X. H., CAVELL, B. E., SYED ALWI, S. S. & PACKHAM, G. 2009. Inhibition of hypoxia inducible factor by phenethyl isothiocyanate. *Biochem Pharmacol,* 78**,** 261-72.
XIAO, D., JOHNSON, C. S., TRUMP, D. L. & SINGH, S. V. 2004. Proteasome-mediated degradation of cell division cycle 25C and cyclin-dependent kinase 1 in phenethyl isothiocyanate-induced G2-M-phase cell cycle arrest in PC-3 human prostate cancer cells. *Mol Cancer Ther,* 3**,** 567-75.
XU, C., SHEN, G., CHEN, C., GELINAS, C. & KONG, A. N. 2005. Suppression of NF-kappaB and NF-kappaB-regulated gene expression by sulforaphane and PEITC through IkappaBalpha, IKK pathway in human prostate cancer PC-3 cells. *Oncogene,* 24**,** 4486-95.
XU, C., YUAN, X., PAN, Z., SHEN, G., KIM, J. H., YU, S., KHOR, T. O., LI, W., MA, J. & KONG, A. N. 2006. Mechanism of action of isothiocyanates: the induction of ARE-regulated genes is associated with activation of ERK and JNK and the phosphorylation and nuclear translocation of Nrf2. *Mol Cancer Ther,* 5**,** 1918-26.
ZHANG, Y. 2000. Role of glutathione in the accumulation of anticarcinogenic isothiocyanates and their glutathione conjugates by murine hepatoma cells. *Carcinogenesis,* 21**,** 1175-82.
ZHANG, Y. 2001. Molecular mechanism of rapid cellular accumulation of anticarcinogenic isothiocyanates. *Carcinogenesis,* 22**,** 425-31.

Appendices

GIALLOUROU, N., ORUNA-CONCHA, M. J. & HARBOURNE, N. 2016. Effects of domestic processing methods on the phytochemical content of watercress (*Nasturtium officinale*). Food Chem, 212, 411-9.

http://www.sciencedirect.com/science/article/pii/S0308814616308792

